SCIENTIA EST POTENTIA

KNOWLEDGE IS POWER

ON THE COVER

DESIGNED BY TEAGAN WHITE

The front cover features the downtown campus of McGill University, nestled at the base of Mont Royal in the heart of Montréal. The river coursing through, an analogue to the Saint Lawrence River, symbolizes the power of research to carve through and transform human and natural landscapes. As well, science, much like a river, acts as a conduit allowing humankind to venture out to unknown territories and follow in pursuit of the great ocean of truth.

THE 2010-2011 MSURJ COMMITTEE

MCGILL SCIENCE UNDERGRADUATE RESEARCH JOURNAL 805 SHERBROOKE ST. WEST ROOM 1B21 MONTRÉAL, QUÉBEC, H3A 2K6 CANADA

P. 514.398.6979
F. 514.398.6766
E. MCGILLSURJ@GMAIL.COM
W. MSURJ.MCGILL.CA

TABLE OF CONTENTS

TABLE OF CONTENTS

FOREWORD

DEAR READER,

Since 2006, the McGill Science Undergraduate Research Journal (MSURJ) has played an integral role in promoting research at the undergraduate level in McGill University. With the publication of our sixth volume, we continue this proud tradition of encouraging students to communicate their efforts and contributions to science.

Since our inaugural edition, we have developed many new partnerships with faculty members and educators outside the McGill community in order to promote science writing. Last year, we established a community outreach program targeting science students at CÉGEPs in the Montréal area. We continued our efforts this year to reach students both inside and outside labs and lecture halls.

As a journal in a leading global research institution, we recognize the importance of establishing national and international partnerships. This year marks a new step towards this goal for MSURJ, as we begin to open up our doors to student research beyond the walls of McGill. By broadening the scope of MSURJ's mandate, we hope to offer a unique venue to undergraduate researchers from across the world to communicate their work to a large audience.

With this issue, we are excited to present you with some of the remarkable work of students at McGill University and elsewhere. Articles in this volume range in focus from environmental sciences to biophysics, vividly demonstrating the diversity of research in science, as well as the quality of research that can be achieved at the undergraduate level.

DANIEL FRIEDLANDER AND MARZIEH GHIASI

EDITORS-IN-CHIEF

ACKNOWLEDGEMENTS

The launch of the sixth edition of the McGill Science Undergraduate Research Journal would not have been possible without the support of many individuals.

We thank Professor Martin Grant, Dean of the Faculty of Science, whose unwavering support throughout the past six years has allowed this journal to flourish.

We thank all of our donors in the McGill community for their generous support.

Biochemistry Undergraduate Society
Department of Atmospheric and Oceanic Sciences
Department of Earth and Planetary Sciences
Faculty of Medicine
Faculty of Science
McGill Anatomy and Cell Biology Students' Society
McGill Biology Student Union
McGill Psychology Students' Association
McGill School of Environment
Monteregian Society

The Science Undergradue Society

We also extend our gratitude to

Mr. Victor Chisholm for providing us with continued encouragement at every step of the way.

Dr. Frédéric Guichard of the Department of Biology for his enthusiasm and support for this initiative.

We wish to thank the professors and post-doctoral fellows who graciously offered their time to review students' article submissions.

We would like to acknowledge the tireless efforts of the MSURJ board of editors in assembling this edition of the journal, as well as the designers whose skills realized our visions. Lastly, we wish to recognize the student contributors whose commendable efforts have made this journal possible.

Pathogenic copy number variants (pCNVs) in individuals diagnosed on the autism spectrum disorder (ASD): A closer look at candidate genes

Allan Dale Baniaga*[1]

[1]Department of Integrated Sciences, The University of British Columbia, 2329 West Mall, Vancouver, British Columbia, Canada V6T 1Z4
Guest Article

ABSTRACT

Introduction: The genetic basis for autism spectrum disorders (ASDs) is well established and its heterogenetic nature provides us with substantial evidence for the many chromosomal aberrations associated with this complex disorder *(5)*. However, little is known about the genes that occupy the different chromosomal regions and the gene networks they participate in as they relate to phenotypes associated with ASDs. **Methods**: Here, the author reports pathogenic copy number variants (pCNVs) validated through array-comparative genomic hybridization (CGH) and the candidate genes found on these affected regions that may be implicated in the observed clinical phenotypes in 9 patients diagnosed with an ASD. Formal clinical assessments, which include a full physical examination, a medical history report, and a family history, were administered by a clinical geneticist unaware of the array-CGH results. **Results**: The author's findings suggest a number of genes involved in neurodevelopment as well as craniofacial and systemic features that may account for the observed phenotypes in the nine affected patients. **Discussion**: Among the candidate genes found, the *CYFIP1* gene, which is involved in maturation and maintenance of dendrites, the Gamma acid receptor family (*GABA*) which exhibit linkage disequilibrium with autistic disorders, and the *PHF8* and *WNK3* genes, which have been shown to be associated with X-linked mental retardation (XLMR), present the most interesting findings as they may account for most of the neurodevelopmental pathogenesis observed in the affected patients. Future studies need to be conducted in order to precisely determine the networks these genes participate in and how they are regulated to gain a deeper understanding in the roles they play in the clinical presentations of affected individuals with ASDs.

KEYWORDS

Autism, chromosome, disorder, genetics, interactions, networks, phenotype

*Corresponding author:
baniaga@interchange.ubc.ca
Received: 25 November 2010
Revised: 28 February 2011

INTRODUCTION

Autism Spectrum Disorders (ASDs) are neurodevelopmental disorders characterized by impairments ranging from communication, social interaction, and repetitive behavior impairments, and have a prevalence as high as 60 per 10,000 individuals by recent estimates *(1-4)*. The heritability of ASDs has also been well established over the years, particularly through the comparison monozygotic (MZ) and dizygotic (DZ) concordance rates that, when examined collectively with family studies, clearly point to an important genetic basis for autism *(5)*. Although current estimates strongly show that clinical genetic evaluation can identify

a specific etiology in up to 40% of individuals with an ASD *(6)*, little is understood in terms of the genotype-phenotype correlations for the vast majority of genetic abnormalities found in affected individuals. The current paper identifies possible candidate genes associated with particular pathogenic copy number variants (pCNVs) in subjects with ASDs, particularly in 3 pairs of individuals, 2 pairs of which had *de novo* changes, and a pair of brothers who inherited the same X-linked deletion from their unaffected mother. Three other individuals with ASDs encompassing impairments in communication, social interaction, and repetitive behavior were also identified to have unique copy number changes not shared with other affected individuals in the cohort. Array-CGH, FISH, and RT-qPCR data were gathered from experiments, as well as detailed phenotypic descriptions from formal clinical assessments by a professional Clinical Geneticist (M.E.S.L.) for these affected individuals. From these, candidate genes in each unbalanced region were compiled through the use of various databases so as to provide a genetic basis for their clinical phenotypes.

METHODS AND MATERIALS

IDENTIFICATION OF PATHOGENIC COPY NUMBER VARIANTS (pCNVs)

A total of nine subjects were identified to have pCNVs through various genetic testing methods. Low resolution array-CGH findings were confirmed by FISH and RT-qPCR methods, which were also used to refine breakpoints and determine the origins of the changes where parents were available for testing.

Individuals identified to harbour pCNVs found at genomic loci associated with other disorders fulfilled CNV criteria strongly suggesting the pathogenicity of their pCNVs *(7)*. Several criteria were used to distinguish benign CNVs (bCNVs) from potentially pathogenic ones (pCNVs), including: a *de novo* origin (or maternally inherited X-linked in male probands), the involvement of multiple genes not known to vary in databases with regards to their expression and function, the overlap with a gene or region that leads to a clinical phenotype when there is a dosage imbalance of the gene product, or if the affected region is >1Mb and overlaps well characterized genes *(7)*, *(8)*. This is in contrast to benign CNVs (bCNVs) which are found in at least two healthy individuals in independent studies found on the Database of Genomic Variants website.

ARRAY-CGH

PUREGENE DNA Isolation Kits (Gentra, Minneapolis, MN) were utilized to extract DNA from the peripheral blood of the nine subjects examined and were matched to normal male and female control DNAs (Promega, Madison, WI) as a reference. Both sample and reference DNAs were then subsequently hybridized using the 1-Mb BAC array *(9)* [Spectral Genomics, Houston, TX] through dye swap methods. Data analysis was conducted with Spectralware 2 software (Spectral Genomics) and clones bearing a significant gain or loss were identified through the use of the experimentally established values of 1.2 and 0.8, respectively, as cut-offs.

FISH

Deletions and duplications of BAC DNA clones identified by array-CGH were confirmed through FISH analyses *(10)*. A Zeiss Axioplan 2 fluorescence microscope and the MacProbe software (Applied Imaging, Santa Clara, CA) were then utilized to view the slides and capture the images, respectively.

REAL-TIME QUANTITATIVE PCR (RT-qPCR)

RT-qPCR *(11)* was employed to confirm the pCNVs. The ABI Prism 7900HT system (Applied Biosystems) using SYBR Green I detection was utilized to assess the RT-qPCR products. The primers used can be made available upon request.

PHENOTYPIC DATA

A spectrum of clinical characteristics modified from the De Vries scoring method were taken into account in identifying the phenotypes, and includes prenatal and postnatal growth abnormalities that are indicative of subtelomeric rearrangements not in exclusion of other characteristics. A spectrum of clinical and physical characteristics was noted for each participant by a professional Clinical Geneticist (M.E.S.L.) blinded to the array results. These include micro- and macrocephaly, prenatal and postnatal growth abnormalities, craniofacial dysmorphisms, systemic anomalies, and the presentation of medical co-morbidities such as seizures, intellectual disabilities (ID), and gastro-intestinal (GI) problems. Pregnancy and postnatal histories were also collected at the time of the appointment.

IDENTIFICATION OF CANDIDATE GENES

A general list of candidate genes were compiled for each proband through the Database of Genomic Variants website (http://projects.tcag.ca/variation/), and were subsequently narrowed down further using the SUSPECTS database (http://www.genetics.med.ed.ac.uk/suspects/). The major premise of SUSPECTS is that genes associated with complex traits will participate in the same gene networks and exhibit similar expression patterns, and the program achieves this by ranking candidate genes according to their possible involvement with the trait of interest. Only candidate genes that SUSPECTS was able to positively confirm as accounting for the observed clinical phenotypes were included in the final list of genes compiled in Figure 1.

Genotype-phenotype relationship information on each candidate gene identified by SUSPECTS was collected through the NCBI

SUBJECT(S)	GENOMIC REGION IN (BP)[2] (START/END)	PATHOGENIC CNV(S) AND CYTOBAND(S)[2]	ORIGIN	CANDIDATE GENE(S)[1]	GENE ONTOLOGY[3]
A, B	**A**=56,800,000/63,200,000 **B**=55,500,000/63,400,000	del 2p15 – 16.1	de novo	**1**.PEX13 **2**.OTX1	**1**.Peroxisome biogenesis disorders **2**.Brain and sensory organ development, inner ear morphogenesis
C, D	**1**. 19,570,792/20,341,734 **2**. 20,536,416/30,830,821	**1.**del 14q11.2 **2**.dup 15q11 – 12	both translocations	**1a**.NP **2a**.NIPA1/NIPA2 **b**.CYFIP1 **c**.NDN **d**.SNRPN **e**.UBE3A **f**.ATP10A **g**.GABRB3 **h**.GABRA5 **i**.GABRG3 **j**.APBA2 **k**.CHRFAM7A **l**.GREM1 **m**.SCG5	**1a**.Purine nucleoside phosphorylase Activity **2a**.Prader-willi/angelman syndrome **b**.Nervous system development **c**.Neuron development **d**.Rna splicing, prader-willi Syndrome **e**.Brain development, angelman Syndrome **f**.Angelman syndrome **g**,**h**,**i**.Gaba-a receptor activity **j**.Nervous system development **k**.Role in failure to thrive in infants **l**.Bone and nervous system Development **m**.Neuropeptide signaling, hormone Secretion regulation
E, F	53,970,960/54,326,640	del xp11.2 (highly skewed x-inactivation)	familial inherited	**1**.PHF8 **2**.WNK3	**1**.X-linked mental retardation **2**.Protein amino acid phosphorylation
G	**1**. 15,780,358/15,940,642 **2.** 9,334,790/11,738,791	**1**.del 3p24.3 – 25 **2**.del 5p15.2	**1.**de novo **2.**de novo	**2a**.SEMA5A **b**.CCT5 **c**.CTNND2	**2a**.Axonal guidance, nervous system Development **b**.Chaperon protein binding **c**.Neuron adhesion, synaptic Plasticity
H	72,200,000/73,767,523	dup 7q11.23	unknown origin	**1**.GTF2I	**1**.General transcription factor, Williams-beuren syndrome
I	5,910,725/6,063,460	dup 18p11.3	de novo	**1**.L3MBTL4	**1**.Cell adhesion, platelet activation, Integrin complex component

Fig. 1. Observed Clinical Phenotypes
[1]Confirmed through Database of Genomic Variants website and subsequently narrowed down with SUSPECTS database
[2]Affected region confirmed by RT-qPCR and/or FISH
[3]Information gathered collectively from the NCBI, iHOP, and metalife databases

website (http://www.ncbi.nlm.nih.gov/), specifically looking at the Entrez Gene record and the database of Genotype and Phenotype (dbGaP) entry (when available) for each gene. Further information regarding genotype-phenotype relationships were gathered from the iHOP website (http://www.ihop-net.org/UniPub/iHOP/) which compiles a list of all known functions, interactions, and diseases the gene of interest is associated with. The metalife database (http://www.phenomicdb.de/) was also utilized to complement the gene ontology information collected from the iHOP website and gives a summary of all the collective research done on a gene of interest as well as linking it to various phenotypes associated with the gene.

RESULTS

Figure 1 summarizes the pCNVs found and validated, the candidate genes for each subject pair sharing the same pathogenic CNV, as well as the candidate genes for individuals bearing unique pCNVs. All candidate genes identified and confirmed by the SUSPECTS database has been reported in full in Figure 1. Known gene ontologies for each candidate gene are also listed in Figure 1. A list of shared and unique phenotypes was also compiled in Figure 2 for each pair and for unique individuals bearing a particular pathogenic CNV. Figure 1 is a schematic diagram summarizing all of the candidate genes found on the various chromosomes.

SUBJECT(S)	GENOMIC REGION IN (BP)[2] (START/END) PATHOGENIC CNV(S) AND CYTOBAND(S)[2] ORIGIN	CANDIDATE GENE(S)[1] GENE ONTOLOGY[3]
A, B	Severe ID[1], microcephaly (<2%), craniofacial dysmorphisms (short forehead, high and broad nasal root), other systemic dysmorphisms (bilaterally tight heel cords, oral motor dysfunction), abnormal brain imaging	**A**=Prenatal growth retardation **B**=Seizure disorder, postnatal small stature (<5%)
C, D	Craniofacial dysmorphisms (strabismus, flat occiput, prominent alar cartilage), no other systemic dysmorphisms	**C**=Moderate ID, respiratory distress and poor suck and feeding difficulties (postnatal) **D**=Mild ID, seizure disorder, floppy infant (postnatal)
E, F	Moderate ID, craniofacial dysmorphisms (flat occiput, coarse asymmetric face [right side > left side fullness], micrognathia, unilateral cleft lip), other systemic dysmorphisms (pes planus, bone anomalies)	**E**=Prominent metopic suture, prominent finger pads **F**=Long slender fingers, macrocephaly at birth, mild hyperoptic refractive error
G	N/A	**G**=Moderate ID, seizure disorder, macrocephaly (>98%), postnatal large stature (>98%), craniofacial dysmorphisms (coarse facial features, frontal bossing, prominent supra-orbital ridge), other systemic dysmorphsims (prominent finger pads, bilateral tight heel cords, slight toe walking)
H	N/A	**H**=Moderate ID, craniofacial dysmorphisms (plagiocephaly, brachycephaly, prognathia), other systemic dysmorphisms (GI unusual dark stool colour, walks on heels, occasional enuresis), normal brain imaging
I	N/A	**I**=Mild ID, hightened blood pressure (during pregnancy), craniofacial dysmorphisms (mild bilateral epicanthal folds, ears bilaterally protuberant, slight malar flattening), other systemic dysmorphisms (slight metatarsus varus when walking)

Fig. 2. Observed Clinical Phenotypes
[1]ID = Intellectual Disability

SUBJECTS A AND B

The affected, unrelated pair share almost identical 2p15-16.1 deletions, both of *de novo* origin. The affected region has been further defined and validated to be from positions 56,800,000 to 63,200,000 for *subject A*, and from 55,500,000 to 63,400,000 for *subject B* on chromosome 2 confirmed through RT-qPCR and FISH methods.

Candidate genes for both subjects within the overlapping regions include *PEX13*, involved in Peroxisome Biogenesis Disorders, and *OTX1*, involved in brain and sensory organ development as well as inner ear morphogenesis.

SUBJECTS C AND D (FAMILY #1)

Subject D is the aunt of *subject C*, and both individuals share the same deletion at the 14q11.2 locus and duplication at the 15q11-12 locus. An unbalanced product of a reciprocal cryptic 14q/15q translocation represents this finding. A perfect overlap has been confirmed at the 14q11.2 and 15q11-12 regions between both subjects (19,570,792 to 20,341,734 and 20,536,416 to 30,830,821, respectively).

Of particular note, several candidate genes are involved in nervous system development, which include *CYFIP1*, *NDN*, *UBE3A*, *APBA2*, *GREM1*, and *SCG5*, all of which are found on the shared 15q11-12 site. Several candidate genes found on the same locus are also clearly involved in Angelman syndrome as well as Prader-Willi syndrome, and includes the *NIPA1*/*NIPA2*, *SNRPN*, *UBE3A*, and *ATP10A* genes.

SUBJECTS E AND F (FAMILY #2)

Subjects E and F are brothers who share the same Xp11.2 deletion that is familial inherited, and the precise genomic region was found and validated to be from 53,970,960 to 54,326,640 on the X chromosome. The mother was confirmed to have a relatively skewed X-inactivation, perhaps implying dosage imbalance problems in both siblings. Potential candidate genes in the affected region of both *subjects E and F* include *PHF8*, which is associated with X-linked mental retardation, as well as the *WNK3* gene, which is involved in protein amino acid phosphorylation.

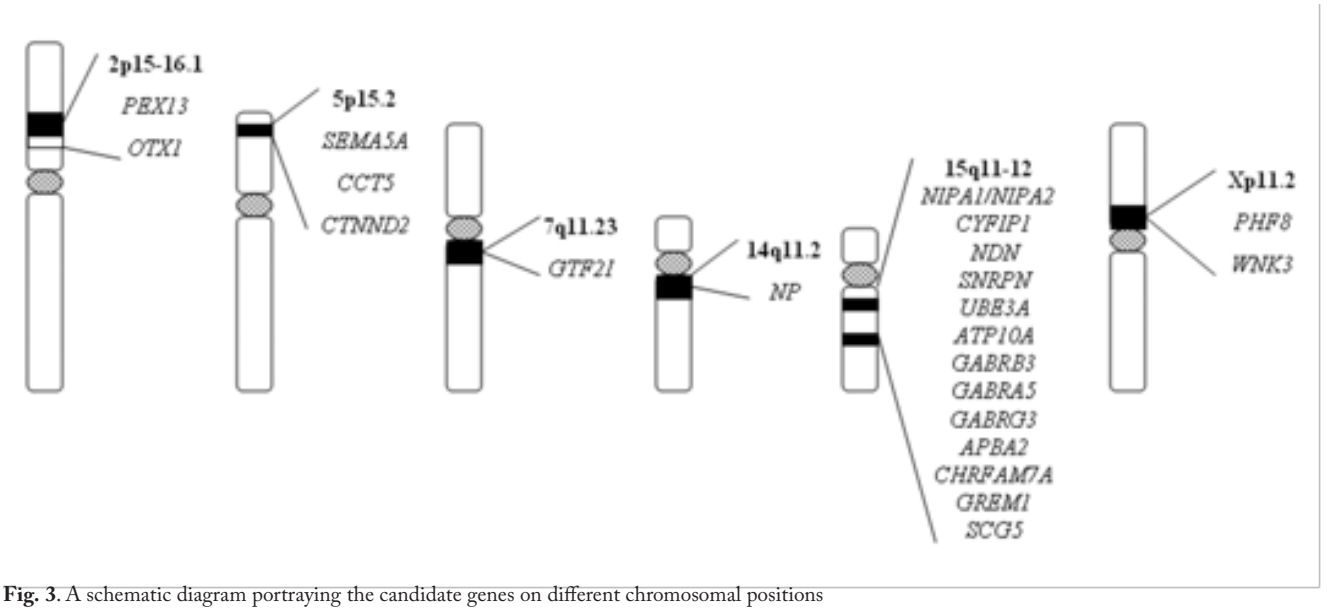

Fig. 3. A schematic diagram portraying the candidate genes on different chromosomal positions

SUBJECT G

The affected individual harbours two deletions at the 3p24.3-25 and 5p15.2 regions, with both regions of *de novo* origin. The precise affected region for the chromosome 3 deletion was confirmed to be from 15,780,358 to 15,940,642, and the chromosome 5 deletion is from 9,334,790 to 11,738,791, as validated by FISH and RT-qPCR.

In relation to the observed phenotypes, several candidate genes located on chromosome 5 that may play a role in the pathogenesis of classical autism include *SEMA5A*, which is involved in axonal guidance, and *CTNND2*, which is involved in neuron adhesion and synaptic plasticity. *CCT5* was also identified by SUSPECTS to be another candidate gene on the same chromosome, and is involved with chaperon protein binding in neurons.

SUBJECT H

Subject H is an individual with a unique 7q11.23 duplication of unknown origin that is not found in other subjects presenting with pathogenic CNVs. The affected genomic region was confirmed to be from 72,200,000 to 73,767,523 through FISH and RT-qPCR methods. Notably, the GTF2I gene was identified as a candidate gene by the SUSPECTS database, and is known to be as a general transcription factor, as well as being implicated in Williams-Beuren syndrome.

SUBJECT I

This affected individual was identified to have a duplication of *de novo* origin at the 18p11.3 region which was further refined to be from 5,910,725 to 6,063,460 on chromosome 18. *L3MBTL4* was the sole candidate gene identified that may account for the observed phenotypes, and is known to be involved in cell adhesion, platelet activation, as well as being a component of the integrin complex.

DISCUSSION

SUBJECTS A AND B: 2P15-16.1 DELETION

Several characteristics shared by both subjects include intellectual disability as well as poor oral motor skills (ie. speech) and poor muscle tone, which overlap with certain Peroxisome Biogenesis Disorders (PBD) phenotypes, thus making the *PEX13* gene on chromosome 2 a possible culprit for the observed phenotypes. Since both subjects are still alive, Refsum's disease is the most likely out of all the other PBDs as its prognosis is the most hopeful in terms of living past the early childhood years. However, both *subjects A* and *B* exhibited normal laboratory evidence of phytanic acid and long chain fatty acids, which are found in elevated levels in Refsum's affected individuals due to faulty enzymes during the alpha oxidation of phytanic acid and fatty acid oxidation *(10)*. Nonetheless, the possibility of *PEX13* contributing to part of the observed phenotypes, in particular those involved with neurodevelopment (in keeping with microcephaly in both subjects) and poor muscle tone, cannot be completely ruled out, as well as other candidate genes in the deleted region.

Another candidate gene that may be responsible for neurodevelopment as well as sensory organ formation is *OTX1*, a transcription factor that was recently found to be essential in cerebellum development *(12)*. The observed large ears in both subjects, relative to the microcephaly, may be in part due to the loss of

function of the *OTX1* gene. Furthermore, evidence suggests that the *OTX1* gene dictates the segregation of the saccule and the utricle during inner ear morphogenesis *(13)*, and thus its loss of function due to the deletion may perhaps be responsible for the hyperacusis observed in *subject A* as well as the bilateral sensorineural loss (mild to moderate in the left ear and slight to mild in the right ear) observed in *subject B*.

SUBJECTS C AND D (FAMILY 1): 14Q11.2 DELETION AND 15Q11-12 DUPLICATION

Both subjects present strikingly similar characteristics, most notably sharing several craniofacial dysmorphisms (strabismus, flat occiput, prominent alar cartilage) and intellectual disability (*subject C* has moderate ID while *subject D* has mild ID). These findings suggest an underlying genomic basis that may be responsible for the shared confirmed pathogenesis, and indeed, both a deletion and a duplication arising through a reciprocal cryptic 14q/15q translocation were found whose affected genomic areas were found to have perfect overlap between the two subjects (Fig. 1).

Candidate genes that may be involved with cephalic development were found in the duplicated 15q11-12 region and, as such, dosage effects may be at play here in terms of over-expression of a particular gene and/or altered regulation of a gene that may exert its effects on adjacent genes involved in the same gene network. The highly conserved *CYFIP1* gene may be one such gene. Through co-localization experiments, there is evidence that the products of the *CYFIP1* gene do indeed interact with *FMRPs* [Fragile X mental retardation proteins] *(14)*. Although the functions of the *CYFIP1* proteins are currently unknown, the extraction of *CYFIP1* proteins at the synaptosome of the distal portion of dendrites suggests that they also interact with the small GTPase *Rac1* where *CYFIP1* proteins also localize *(14)*. *Rac1* is known to be essential for dendritic spine maturation as well as maintenance *(15)*, and a duplication of the *CYFIP1* gene with which it interacts may have direct or indirect effects on the maturation and maintenance of these structures. One possibility is that an increased dosage of the *CYFIP1* gene product could directly alter expression levels of *Rac1* and other genes in the network involved in dendrite formation. This would have major implications for neurodevelopment and could thus be responsible for the shared ID and ASD observed in both subjects.

Several other candidate genes that may be responsible for the shared dysmorphisms include *UBE3A* and *APBA2*. Most notably, maternally derived duplications of the 15q11-13 region results in changes to *UBE3A* expression observed in autistic individuals, whereas the duplication is not present in normal individuals *(16)*. In addition, *GREM1* may also be the culprit gene for the observed bone fractures in *subject D* and the ligamentous laxity in *subject C*, as over-expression of the gene in transgenic mice analogous to that of a duplication event resulted in a 20-30% reduction in bone mineral density as well as formation of bone fractures *(17)*. It has been well established that deletions in the 15q11-13 region result in Prader-Willi syndrome (PWS) as well as Angelman syndrome (AS) *(18),* in which several of the phenotypes overlap with those present in both subjects. These include reduced fetal movements, respiration and feeding difficulties, strabismus, and intellectual disability *(19)*. *NIPA1/NIPA2*, *NDN*, *SNRPN*, *UBE3A*, *ATP10A*, and the Gamma acid receptor family (*GABA*) were identified and validated by SUSPECTS in the duplicated 15q11-12 region to be implicated in ASD in both subjects. There is evidence that a marker in the gene for the gamma aminobutyric acid receptor subunit of *GABRB3* was found to have linkage disequilibrium with autistic disorder, making this gene as well as other members of the gene family another prime candidate gene *(20)*. Furthermore, the role of benzodiazepine as a *GABA* receptor agonist in treating autistic phenotypes such as anxiety disorders and seizures suggest a potential role of the *GABA* gene family in the presentation of these phenotypes beyond the normal inhibitory neurotransmitter *GABA* function (20). Additional studies need to be conducted to precisely dissect the roles of the GABA gene family as well as others that exhibit linkage disequilibrium with autistic disorders.

SUBJECTS E AND F (FAMILY 2): XP11.2 DELETION

Both brothers share the same familial inherited Xp11.2 deletion, and a possible candidate gene that may account for the shared moderate ID is *PHF8*. The *PHF8* gene encodes a PHD finger protein that, when mutated through truncation mutation experiments, has been shown to cause X-linked mental retardation (XLMR) with or without cleft lip/cleft palate presentation *(21)*. The PHD finger protein has also been thought to regulate and modify chromatin structure *(22)*, which has major implications in terms of altered transcription levels in neurons and their maturation in individuals with mutations or deletions of the *PHF8* gene.

Another candidate gene that may account for the observed moderate ID in both subjects is *WNK3*, as it has been shown to occupy the critical linkage region on Xp11.2, and thus may also play a critical role in neurodevelopmental disorders such as XLMR *(23)*. However, future studies need to be conducted to determine whether the *WNK3* deletions could account for the difference in autism occurrences in comparison to the *PHF8* deletion cases, and whether deletion size differences between the *WNK3* and *PHF8* genes affect their interaction with neighboring genes.

SUBJECT G: 3P24.3-25 AND 5P15.2 DELETIONS

Subject G is an affected individual identified and validated to harbour unique deletions at the 3p24.3-25 and 5p15.2 regions. Several phenotypes unique to *subject G* include moderate ID, macrocephaly (>98%), postnatal large stature (>98%), and several craniofacial dysmorphisms (coarse facial features, frontal bossing). *SEMA5A*, a candidate gene in the 5p15.2 region identified by SUSPECTS, may account for the observed moderate ID and macrocephaly as it is known to be involved in axonal guidance and nervous system development *(24)*. Experimental evidence in the literature also shows that axonal development and formation of synapses may be affected by changes in *SEMA5A* expression *(25)*. Furthermore, deletions from the 5p band are also implicated in the Cri-du-chat phenotype, and haploinsufficiency of *SEMA5A* may be responsible for the intellectual disability (ID) in individuals exhibiting this phenotype *(26)*. A deletion at the 5p15.2 region may thus have a major impact on *SEMA5A* expression levels as not enough protein is made to maintain proper axonal development and synapse formation, possibly leading to the observed macrocephaly and moderate ID in *subject G*.

CCT5 is another candidate gene that was identified by SUSPECTS to be likely involved in neurodevelopment as the chaperon protein product of *CCT5* was found to have a role in polymerization of cytoskeletal proteins and their structural maintenance in neurons *(27)*. Deletions in the 5p15.2 region would thus have profound effects on proper neurodevelopment due to a lack of *CCT5* chaperone proteins essential for proper neuron functioning. The *CTNND2* gene, which is also found on 5p15.2, was also identified as a possible candidate for the shared macrocephaly and moderate ID phenotypes. Mutational experiments in the literature suggest a specialized role for the *CTNND2* protein as deletions in the gene result in problems in synaptic plasticity in neurons which may lead to learning deficits *(28)*. Furthermore, a strong correlation between a hemizygous deletion of the *CTNND2* gene and severe mental retardation in individuals with Cri-du-chat syndrome (*CDCS*) was found *(29)*, further underlying the critical role of *CTNND2* in intellectual disability in subjects with *CDCS* harbouring a deletion in the 5p15.2 region. Moreover, delta catenin (the protein product of *CTNND2*) was also found to co-bind with kaiso to the promoter sites of rapsyn, a synapse protein necessary for segregating acetylcholine receptors at the neuromuscular area *(30)*.

Deletion of the *CTNND2* gene on 5p15.2 would thus have adverse effects on proper rapsyn functioning, which may in turn contribute to the seizures, delays in motor milestones, as well as failure to thrive observed in the affected individual.

SUBJECT H: 7Q11.23 DUPLICATION

Subject H is an isolated case that does not share any pathogenic CNVs or cytogenetic bands with the other cases here but, nonetheless, the subject's candidate genes have been reported here, as they present distinctive findings. A unique 7q11.23 duplication of unknown origin was found, and *GTF2I* was the sole candidate gene identified by SUSPECTS that may account for the unique phenotypes observed such as plagiocephaly, brachycephaly, and prognathia linked to this affected genomic region. Structural features of 7q11.23 render this region susceptible to genomic rearrangement and deletions, yielding various CNVs that are also involved with Williams-Beuren syndrome (WBS) *(31)*. Several characteristics are shared by the subject with WBS including intellectual disability, hyperacusis, and genito-urinary problems (subject has a history of enuresis) *(32)*. Furthermore, *GTF2I* was also shown to be involved in tooth development at the bud and early bell stage *(33)*, and thus may also account for the carious as well as early loss of teeth in the subject. Moreover, hemizygosity of *GTF2I* was found to be sufficient to account for a number of features associated with WBS, including visuospatial deficits *(34)*, which may contribute to the astigmatism and myopia observed in *subject H*.

SUBJECT I: 18P11.3 DUPLICATION

The affected subject harbours a unique duplication at the 18p11.3 region of *de novo* origin and presents several phenotypes that may be associated with the duplication. Most notably, the candidate *L3MBTL4* gene is known to be involved in platelet activation, and a dosage imbalance arising through a duplication may have direct or indirect consequences with regards to the observed heightened blood pressure during pregnancy. The role of the *L3MBTL4* gene in cell adhesion, in particular as a component of the integrin complex (which is known to be involved in mediating various intracellular signals), may indeed account for the craniofacial and systemic dysmorphisms as well as the mild ID observed in *subject I*. The implications of dosage effects through duplication of the 18p11.3 region need to be further investigated as well as the specific roles of *L3MBTL4*, as research on this region and its genes is limited to make any conclusive statements regarding genotype-phenotype relationships at this time.

CONCLUSION

By identifying and compiling a list of candidate genes on various chromosomes, changes occurring at the gene level affecting phenotype at the organismal level are better understood. This provides us with an overall map of the candidate genes and their respective protein products that may account for the presentation of ASD phenotypes. Autism spectrum disorders present an especially daunting task, as their varied phenotypes between different indi-

viduals suggests a multitude of genes that may interact with other candidate genes involved in the same or different gene networks. Every effort was made to account for the clinical manifestations of the patients presenting with an ASD with their candidate genes through the extensive use of databases in order to hypothesize and explore their genotype-phenotype relationships. In addition to this, the SUSPECTS database utilized in narrowing the list of candidate genes in this paper has limitations in that the matches for the genes are weighed differently for different types of matches. The weights assigned are arbitrary, and so there is concern with regards to how consistent and accurate the program ranks the candidate genes. Additional experiments need to be conducted in the future so as to uncover the functions of these candidate genes, how their expression is regulated, and what gene networks they participate in in order to fully validate or reject their involvement in the observed clinical phenotypes compiled in this paper. The author urges for further research on candidate genes identified in this paper involved in neurodevelopment, which include the Gamma acid receptor family (*GABA*), the *CYFIP1* gene, and the the *PHF8* and *WNK3* genes. Possible experiments that can be conducted in order to further investigate their functions include gain and loss of function experiments to explore the effects of protein dosage on phenotype expression, mutational experiments (such as recessive mutations in hemizygosity), stoichiometry and amplification experiments, as well as looking at the three-dimensional nuclear structure of the chromosomal regions involved. Only through understanding the finer details at the gene level through further experimental research can we then unravel the genetic bases for some of the phenotypes associated with classical autism.

ACKNOWLEDGEMENTS

The author would like to thank Noemie Riendeau and Ying Qiao at the Child and Family Research Institute (CFRI) wet lab for all of their help in assisting with the CNV data, as well as for their insightful comments. A warm thank-you also goes out to Priscilla Carrion and Lindsay Swinton at the dry lab for all of their help with the clinical files, all of which the author is grateful for having access to. And last, but certainly not least, the author would like to express his sincerest gratitude towards his mentor, Dr. Lewis, for allowing the author to undertake this directed studies project, as well as for all of her guidance without which this project would have never been possible without.

REFERENCES

1. G. Baird, T. Charman, S. Baron-Cohen, A. Cox, J. Swettenham *et al. J. Am. Acad. Child Adolesc.* **39**, 694–702 (2000).
2. J. Bertrand, A. Mars, C. Boyle, C. Bove, M. Yeargin-Allsopp *et al. Pediatrics*. **108**, 1155–1161 (2001).
3. S. Chakrabarti and E. Fombonne, *JAMA*. **285**, 3093–3099 (2001).
4. S. Chakrabarti and E. Fombonne, *Am. J. Psychiatry*. **162**, 1133–1141 (2005).
5. C.J. Newschaffer et *al. Annu. Rev. Public Health*. **28**, 235–258 (2007).
6. G.B. Schaefer and N.J. Mendelsohn, *Genetics in Medicine*. **10**(1), 4-12 (2008).
7. Y.S. Fan, P. Jayakar, H. Zhu, D. Barbouth, S. Sacharow *et al. Human mutation*. **28**(11), 1124-1132 (2007).
8. C. Lee, A.J. Iafrate, A.R. Brothman, *Nat. Genet*. **39**, S48-54 (2007).
9. C. Tyson, C. Harvard, R. Locker, J.M. Friedman, S. Langlois *et al. Am. J. Med. Genet. A*. **139**(3), 173-185 (2005).
10. E. Rajcan-Separovic, C. Harvard, X. Liu, B. McGillivray, J.G. Hall *et al. J. Med. Genet*. **44**(4), 269-276 (2007).
11. Y. Qiao, X. Liu, C. Harvard, S.L. Nolin, W.T. Brown *et al. BMC genomics*. **8**, 167 (2007).
12. T. de Haas *et al. J. Neuropathol Exp. Neurol*. **65**(2), 176-186 (2006).
13. K.W. Beisel *et al. Journal of Vestibular Research*. **15**(5-6), 225-241 (2005).
14. A. Schenck *et al. PNAS*. **98**(15), 8844-8849 (2001).
15. A.Y. Nakayama, M.B. Harms, L. Luo, *The Journal of Neuroscience*. **20**(14) 5329-5338 (2000).
16. J. Veenstra-VanderWeele, D. Gonen, B.L. Leventhal, E.H. Cook Jr, *Mol. Psychiatry*. **4**, 64-67 (1999).
17. E. Gazzerro *et al. Endocrinology*. **146**(2), 655–665 (2005).
18. B. Dittrich *et al. Hum. Genet*. **90**, 313-315 (1992).
19. V.A. Holm et *al. Pediatrics*. **91**, 398-402 (1993).
20. E.H. Cook Jr. *et al. Am. J. Hum. Genet*. **62**, 1077–1083 (1998).
21. F. Laumonnier *et al. J. Med. Genet*. **42**, 780–786 (2005).
22. L.R. Jensen *et al. Am. J. Hum. Genet*. **76**, 227–236 (2005).
23. H.H. Ropers *et al. Trends Genet*. **19**, 316-320 (2003).
24. R.H. Adams, H. Betz, A.W. Puschel, *Mech. Dev*. **57**, 33–45 (1996).
25. L. Jones, G. Lopez-Bendito, P. Gruss, A. Stoykova, Z. Molnar, *Development*. **129**: 5041–5052 (2002).
26. A.D. Simmons, A.W. Puschel, J.D. McPherson, J. Overhauser, M. Lovett, *Biochem. Biophys. Res. Commun*. **242**, 685–691 (1998).
27. G.J. Bourke, W. El Alami, S.J. Wilson, A. Yuan, A. Roobol *et al. J. Neurosci. Res*. **68**: 29–35 (2002).
28. I. Israely *et al. Curr. Biol*. **14**, 1657–1663 (2004).
29. M. Medina, R.C. Marinescu, J. Overhauser, K.S. Kosik, *Genomics*. **63**(2), 157–164 (2000).
30. M. Rodova, K.F. Kelly, M. VanSaun, J.M. Daniel, M.J. Werle, *Mol. Cell Biol*. **24**(16), 7188–7196 (2004).
31. I. Cuscó, R. Corominas, M. Bayés *et al. Genome Res*. **18**(5), 683-694 (2008).
32. Z. Sammour, C. Gomes, R. Duarte, F. Trigo-Rocha, M. Srougi, *The Journal of Urology.* **175**(4), 1472-1476 (2006).
33. A. Ohazama and P.T. Sharpe, *Developmental Dynamics*. **236**(10), 2884–2888 (2007).
34. L. Edelmann *et al. Journal of Medical Genetics*. **44**, 136-143 (2007).

Equilibrium dynamics of single DNA molecules confined to nanopit structures

Hugo B. Brandao*[1], Walter Reisner[2]

[1,2]Department of Physics, McGill University, 3600 rue University, Montreal, Quebec, Canada H3A 2T8

ABSTRACT

Introduction: Of great interest in the physical sciences today, is the study of single molecules in nano-fluidic devices. These 'labs-on-a-chip' can provide the basic framework for quantifying the behavior of molecules, such as polymers, under confinement. This study is an investigation of a theoretical free-energy model used to predict thermodynamic properties of DNA molecules situated in a device called a nanopit array. Two parameters in the model, molecule length and nanopit width, are varied and tested against experimental data. **Methods**: Video-fluorescence microscopy was used to image single DNA molecules in the nanopit array; analysis consisted of determining the average number of nanopits occupied by a single DNA molecule over time. **Results**: Good qualitative agreement was reached between theory and experiment for the nanopit width variation, but molecule-length variation predictions were shown to still need improvement. A least-squares fit of the theory to the data suggested that the entropic parameter, A, and the excluded volume term, B, have a modified dependence on nanoslit height and nanopit depth than what is currently predicted by the model. **Discussion**: These experiments confirm that the theoretical model is adequate under certain regimes and predicts conditions under which theory and experiment may significantly diverge. Modifications to the theory are proposed.

KEYWORDS

DNA, nanopit array, fluorescence video-microscopy

*Corresponding author:
hugo.brandao@mail.mcgill.ca

Received: 2 January 2011
Revised: 13 March 2011

INTRODUCTION

Serious theoretical treatment of the fundamental behaviour of polymers began in the late 1960's and early 1970's with some groundbreaking scaling arguments by de Gennes *(1)* and Edwards *(2)*. It has only been in recent years *(3)*, with the advances in nano/microfabrication techniques, that emerging nano-fluidic devices such as nanopores, nanochannels, and nanoslits have been able to rigorously test some of these early theoretical models *(1,2)*.

Recent experiments have probed the effects of geometric confinement on individual DNA molecules in one-dimensional nanochannels *(3,4)* and in two dimensional nanoslits *(5,6)*. When the walls of the nano-fluidic device confine the DNA below its bulk characteristic size in solution (i.e. the radius of gyration), both the static and dynamic behaviour *(6)* of individual molecules is altered due to the steric interactions of the DNA with its confining walls, as well as the hydrodynamic self-interactions.

This study is a further exploration of a new kind of nano-fluidic device, the nanopit array, developed initially by Reisner *et al. (7)* in 2008. Nanopit arrays are nanoslits, which consist of a thin slit between two wafers with a lattice of embedded nanopits on the bottom wafer, as seen in Fig. 1. A DNA molecule confined to a nanopit will assume a stable configuration that minimizes its free-energy. In its search for a state of equilibrium, a given DNA molecule will either fill a single nanopit or span multiple nanopits depending on its contour length *L* and geometric parameters such as slit height *h*, pit depth *d*, pit width *a*, and pit spacing *l*. When a molecule spans multiple pits, the amount of molecule in a given pit fluctuates in time as molecules exchange contour back and forth due to Brownian fluctuations *(7)*.

From a technological point of view, nanopit arrays provide a simple way to manipulate single DNA molecules on a chip, providing more flexibility and precision than conventional nanoslits, and more degrees of freedom than nanochannels. For example, it is possible to imagine - using nanopit arrays in conjunction with embedded nanopores in each pit - that one could perform highly localized chemistry on a particular appealing segment of DNA or some generic polymer. Furthermore, nanopits may be useful in applications such as single-molecule denaturation mapping in nano-fluidic channels *(8)*. For instance, if nanopits were etched into a nanochannel, they might serve as local reservoirs for temporarily unneeded molecule segments, while the segments of DNA undergoing analysis extend into the nanochannel. Once a given segment has been analysed, pressure can be applied to drive contour from the reservoir into the nanochannel and to shift the analysed contour segment into an adjacent reservoir.

The aim of this paper is to test the free-energy model presented by Reisner *et al. (7)*. With this model, it is possible to predict thermodynamic quantities from a chip's geometry and DNA molecule properties. By separately varying the DNA molecule's length *(L)* and nanopit width *(a)*, experimental data was gathered using fluorescence video-microscopy of single λ-DNA molecules in the nanopit arrays; the data was analyzed using the numerical programming package, MATLAB.

The viral DNA molecule (λ-DNA) was used in this experiment to allow for experimental comparison to previous work done by Reisner *(7)* and to extend his previous work. Measurements of the average number of nanopits occupied by a molecule versus pit width were carried out for a width range of 250-1000nm and compared to the model's predictions. A similar analysis was performed for molecule-length variation using a λ-DNA digest. The integrated intensity of each fragment was used to determine molecule length and a plot of the average nanopit occupancy versus molecule size was made. Using this method, occupancy probabilities were tested against the theoretical predictions for two different parameters in the current model.

BACKGROUND

THEORY FOR OCCUPANCY STATISTICS

Consider a DNA molecule of length *L* constrained to occupy *N* nanopits in a 2D lattice. Next, assume that each pit contains an equal amount of DNA. A molecule can arrange itself in several different ways on the lattice depending on the number *N*; the upper and lower bounds of *N* are set by the physical limitations of its stretching and compressing within the nanopit lattice.

Now, as a consequence of the discrete number of occupied nanopits, the number of energy states accessible to a molecule is effectively quantized. For a particular geometry, the molecule will favour arrangements in a certain number of N nanopits more than others. Provided a model *(7)* to quantify the free energy (ΔF_{tot}) of a molecule within the nanopit array as a function of *N*, the probability, P_N, that *N* pits are occupied can be calculated from

$$P_N = \frac{\Omega_N e^{\frac{-Ftot(N)}{k_B T}}}{\sum_N \Omega_N e^{\frac{-Ftot(N)}{k_B T}}} \qquad [1]$$

Ω_N, the degeneracy, is the total number of different ways of assembling a molecule, in a self-avoiding manner, on a square lattice with *N* occupied pits; it represents the number of states with the same energy. Values for Ω_N can be found in literature *(9)* for N=1 up to N=28. k_B and *T* are Boltzmann's constant and temperature respectively.

The molecule's dynamics should be Brownian in the absence of external sources of fluid flow such as applied electric fields or pressure gradients *(10)*. Hence, it can be rationalized that since adjacent nanopits are identical, each pit contains approximately an equal amount of DNA. Thus, the total contour length *L* can be subdivided into the amount of contour within each pit (L_p), and the amount in the nano-slit, in between the pits, (L_s) to obtain

$$L = N L_p + (N-1) L_s \qquad [2]$$

The change in free energy from *(7)* is then given by

$$\Delta F_{tot} = N\left(F_p - F_s\right) + \left(N-1\right) F_{spring} \qquad [3]$$

(F_p - F_s) is the difference free energy of contour L_p placed in a nanopit versus in a nanoslit, and F_{spring} is an energy term

accounting for the free-energy required to stretch the DNA molecule between nanopits. From a series of polymer theory scaling arguments, F_p - F_s can be re-written as

$$F_p - F_s = -AL_p + BL_p^2 \qquad [4]$$

The parameters *A* and *B* depend on the geometric restrictions of the nanopit array *h*, *d*, *a*, (Fig. 2A) and properties of the DNA molecule, including its persistence length P (the minimum length-scale for which a segment of DNA cannot self-interact) and the width of the molecule *w*. The spring energy *(7)* is given by,

$$\Delta F_{spring} = \frac{l^2}{2PL_s}\left(1 + \frac{1}{2(1 - l/L_s)}\right) \qquad [5]$$

Minimization of the free energy in Eq.3 after the appropriate substitutions of equations 2, 4, and 5, yields the equilibrium value of L_p. Substitution of this value back into Eq.3 determines the equilibrium free energy; curves for the occupancy probability can then be generated by varying one parameter (such as *L* or *a*). Finally, the average pit occupancy for a molecule will be given by

$$n_{avg} = \sum_N N \cdot P_N \qquad [6]$$

EXPERIMENTAL METHODS

EXPERIMENTAL PROCEDURE

Data was collected for fluorescence video-microscopy using a Nikon Eclipse Ti-U inverted microscope equipped with an Andor iXON camera capable of single-photon detection and a 100× 1.4 N.A. oil-immersion objective lens. Nanopit depth and slit height of sample nanopit arrays were measured to be 71±2 nm and 69±2 nm respectively with a profilometer. SEM micrographs of the nano-fluidic chip reveal the pit widths to be 250nm, 300nm, 350nm, 400nm, 500nm, 600nm and 1000nm. These measurements had a 4.4% fractional error at the 95% confidence level as determined from image analysis of the SEM micrographs. Spacing in between pits was fixed at 1 μm for all experiments conducted. Figures 2B and 2C show sample scanning electron microscope (SEM) images of an array of nanopits consisting of 1 μm pit-to-pit spacing and 300nm pit width in typical square lattice geometry.

A silica nano-fluidic chip containing a series of nanopit arrays of varying geometry was held on a chuck by an aluminum retaining ring. Application of pneumatic pressure to run the DNA from the loading reservoirs into the nanopit arrays was ensured by the O-ring seals. Figure 3 shows a schematic diagram of the experimental setup.

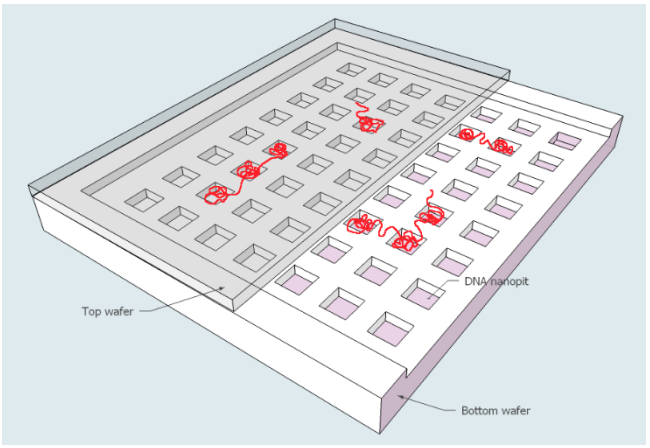

Fig. 1. Three-dimensional schematic diagram of nanopit array. In red is a representation of DNA molecules in the nanopits. The nanopit arrays were constructed on fused silica wafers using a combination of electron beam and UV contact lithography.

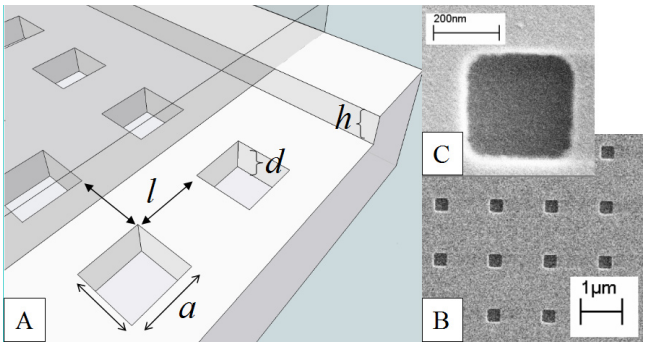

Fig. 2. Close-up view of nanopits in a chip. A) Outline of the important geometric parameters required in the theory to predict DNA occupancy states: slit height (*h*), pit width (*a*), pit depth (*d*), and pit spacing (*l*). B,C) SEM micrograph of an array of nanopits with 1μm pit-to-pit spacing and 300nm pit width.

The DNA was suspended in 10 mM Tris buffer measured at a pH of 7.92±0.02 and a conductivity of 0.53±0.02 mS. The experiment was run using λ-phage DNA (48.5kbp) from New England BioLabs stained with YOYO-1 fluorescent dye (Invitrogen) with a DNA base pair to dye concentration of 5:1. Due to the staining process, the length of the DNA molecule was estimated to increase from 16.5μm to 21μm as was measured by Reisner *et al.* in 2007 *(4)*. To repress photobleaching of the dye and photo-knicking, β-mercaptoethanol was added to the buffer to create a 2% volume/volume solution.

Before conducting the experiment, both the buffer solution and a buffer-filled chip containing the nanopit arrays were left to de-gas overnight. Thus, flow-inducing air bubbles in the microchannels of the chip were effectively removed. Approximately 20μl of the

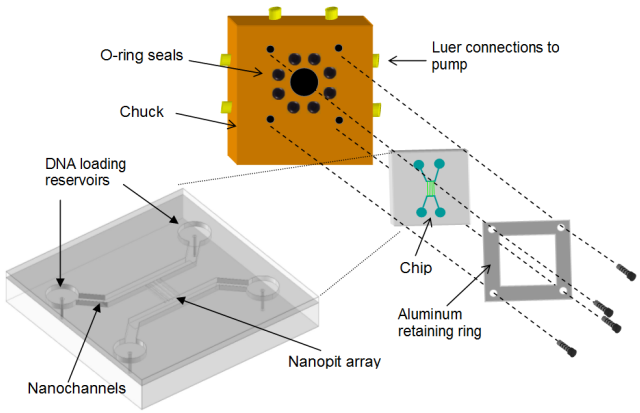

Fig 3. Schematic diagram of chuck and chip. DNA is loaded into the circular loading reservoirs using a micropipette and run with pneumatic pressure ensured via o-ring seals. Small bursts of pressure can be applied to drive DNA from the nanochannel into the nanopit arrays to be imaged. Diagram reproduced but modified from (4) with permission by the author.

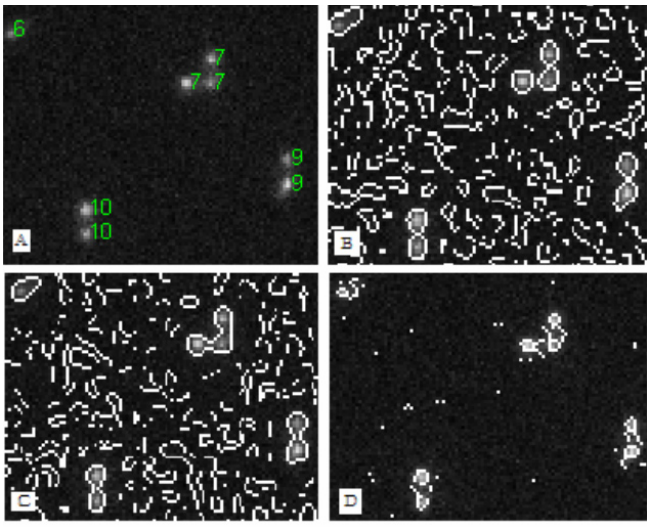

Fig 4. Comparison of various edge-detection techniques available for image analysis. A) Unprocessed fluorescence video-microscopy image taken of λ-DNA molecules; exposure time is 0.1s. B) Edges found via the Laplacian of Gaussian method using an unprocessed image. C) Edges found via the Laplacian of Gaussian method using processed images averaged over three frames. D) Edges found via the Sobel edge-detection method.

prepared DNA/buffer solution was manually loaded the next day with a micropipette into each of the four reservoirs on the chip. 100-200 mbar of pneumatic pressure was used to drive DNA from the reservoirs into the nanoslit to avoid fragmentation of the molecules. Short bursts of 1000-1500 mbar of pressure were then applied to each of the four reservoirs individually to equalize the fluid levels and to minimize unwanted flow. Molecules were allowed to relax in the nanopits for 30-40 seconds after being driven into the nanoslit. Data was acquired continuously by the CCD camera with 100-200 ms exposure times, in frame transfer mode, with negligible delay between image acquisitions. Experiments were conducted at room temperature.

DATA ANALYSIS

Images of the DNA molecules were analysed using MATLAB. A rectangular lattice of square boxes was aligned to the nanopits by the user via a graphical user interface. Occupancy of a nanopit was then established by determining the average pixel intensity value within each box; if the mean intensity within a box was above a certain threshold, then the pit was deemed filled. The threshold parameter was adjusted manually for each image sequence; this flexibility allowed the user to chose the most appropriate value for a given experimental condition and quality of image. Figure 4A shows a typical video-microscopy image of the DNA molecules in the nanopit arrays. Occupied nanopits have all been identified and each nanopit is registered to a particular molecule (indicated by the numbering of each pit).

To distinguish between two molecules in adjacent nanopits, the program relied on an edge-detecting function available in the MATLAB library. This function worked by applying a Gaussian filter to the image via standard convolution methods and a Laplacian operator to detect areas of rapid intensity changes. The algorithm would output an image with the boundary of a molecule clearly defined. If two adjacent nanopits were enclosed by such a boundary, then a single molecule occupied both pits; otherwise, the pits were occupied by different molecules.

The Laplacian of Gaussian method of edge detection performed very well locally. Due to its local nature, it quickly enhanced noise as is evident in figures 4B and 4C; nevertheless, it remained the preferred method of edge detection. Other edge-finding methods were considered including the Roberts and Sobel methods *(11)*. While they often found the DNA molecule edges and did not enhance noise, they failed to produce a smooth, *closed* contour of the whole molecule as can be seen in comparing figure 4D to figure 4B and 4C.

An issue inherent in the short exposure times of 100 ms (used to acquire a detailed profile of the pit-to-pit contour fluctuations of a molecule) was that molecule segments in between pits occasionally disappeared from certain frames. For instance, the bottom left nanopit occupied by molecule 7 in figure 4B appeared disconnected from the other two pits. However, inspection of a sequence of images revealed that all three nanopits belonged to the same molecule.

An approach that proved to be very effective to remedy this kind of problem was to perform image averaging: Each image from the video was averaged with the image in the frame before and

after it before undergoing analysis by the edge-detection algorithm. As an example of the effectiveness of this technique, compare molecule 7 in figure 4B to figure 4C: the link that was previously not apparent has been intensified and picked up by the Laplacian of Gaussian edge-detection algorithm.

To justify the use of frame-averaging, we investigated the timescale for the contour fluctuation of a molecule in between two nanopits: averaging was warranted as long as the time-scale was below the correlation time of pit-to-pit contour fluctuations. By integrating the pixel intensities of each nanopit registered to a series of user-defined boxes, the fluorescence of each pit was found. Then, the correlation coefficient was computed at a series of time lags using the GARCH model (11) for the cross-correlation of integrated intensity between two adjacent pits.

The cross-correlation plots for the integrated intensity of each nanopit were used to determine that, at 95% confidence, it takes between five to ten frames (0.5-1.0s) for contour fluctuations to become uncorrelated. What this signifies is that it takes 5-10 frames for the contour segment in one pit to have no memory of a significant fluctuation that occurred in the adjacent pit. Our frame-averaging combined images for 0.3s, which is 40% less than the smallest observed correlation time, suggesting that we can use frame-averaging without much worry. Figure 5 shows a sample of this result.

RESULTS AND DISCUSSION

JUSTIFICATION OF THE ASSUMPTION OF EQUAL CONTOUR PER NANOPIT

In Section II, the quantization of the energy states of a molecule was introduced by assuming equal amount of molecule per nanopit. This theoretical assumption was initially justified by claiming that all the nanopits were identical; thus, a DNA molecule should fill all nanopits equally. Experimental analysis of seven randomly selected molecules shows that for time intervals taken at least ten times greater than the average correlation times for pit-to-pit fluctuations, nanopits do indeed contain an equal amount of contour to within 4%. The percentage error between the mean pit intensity (within a single user-defined box, i) and the averaged mean intensity for all nanopits occupied by a molecule was computed by:

$$\%\,\text{error}(i) = \frac{X_i - \overline{X}}{\overline{X}} \times 100\% \qquad [7]$$

X_i is the mean intensity of nanopit i and $\overline{X} = \sum_{i=1}^{N} X_i / N$ is the averaged mean intensity.

VARIATION OF MOLECULE LENGTH

It is known that molecule intensity should vary linearly with contour length if the DNA is uniformly stained with an appropriate dye *(8)*. Consequently, when analysing the video-microscopy images for a λ-(mono) DNA digest (New England BioLabs), it was possible to estimate the length of each fragment by using a simple ratio. The nanopit array geometry under analysis consisted of 1 μm pit-to-pit spacing, 100 nm pit depth and slit height, and 300 nm pit width. The experimental fluorescence video-microscopy images were collected by Reisner at the Technical University of Denmark and were processed and analysed with his permission.

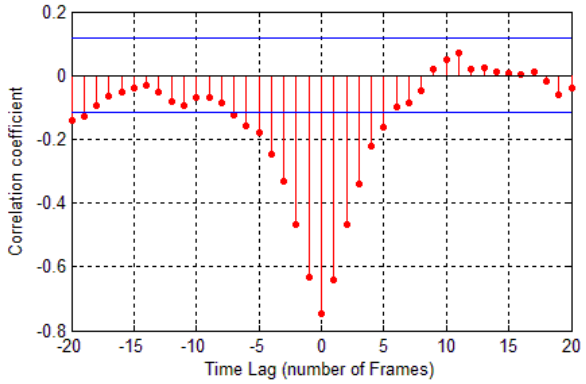

Fig 5. Sample cross-correlation plot of pit-to-pit contour fluctuations of a DNA molecule in a nanopit array with geometry l=1μm, a=300nm, h=d=100nm. Correlation coefficients within the horizontal blue bars delimit uncorrelated data to within a 95% confidence level.

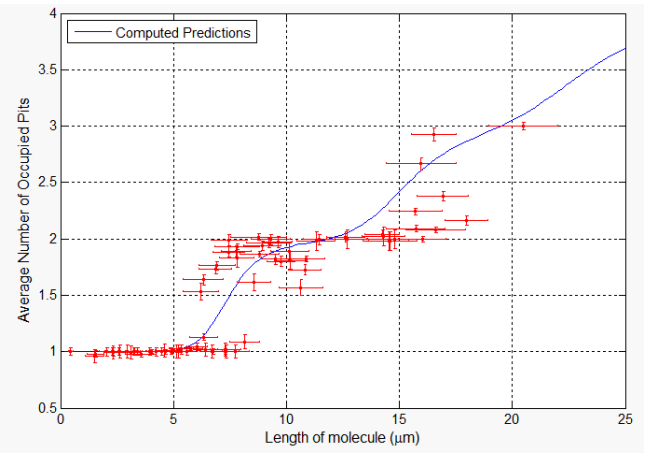

Fig 6. Average nanopit occupancy of a digest of λ-DNA fragments in a nanopit array of dimensions a=300nm, h=d=100nm, l=1μm. Error bars are reported for both the intensity and occupancy at 68% confidence. The solid line is the theoretical prediction for n_{avg} as a function of contour length.

The ratio of pixel intensity to contour length was calibrated using values from previous experiments *(7)*, where it is shown that a full-length λ-DNA molecule occupies on average 3.2±0.1 nanopits. In this experiment, the molecule exhibiting the greatest average occupancy state for the DNA digest (n_{avg} = 3.01±0.05) was taken to be 21 μm long. The two results are not comparable within error; however, for the purposes of qualitative comparison of the data to the theory, the difference is small enough to ignore.

Average pit occupancy was plotted against contour length for 82 different molecules together with the theoretical predictions. The theoretical curve was obtained from using the values for the persistence length *P*, chain thickness w, and geometric parameters of the chip used by Reisner *et al.* in the 2008 study *(7)*. As observed in figure 6, the average occupancy varies very non-linearly with contour length in what appears to be a series of steps. While the theoretical curve seems to follow the general trend of the molecule's distribution, it seems to first underestimate then overestimate the average occupancy at the transitions between n_{avg} states occurring at *L*=7.5 μm and *L*=17 μm respectively. Moreover, the average nanopit occupancy at around 17μm increases very suddenly from n_{avg}=2 to n_{avg}=3. This sharp transition in the experimental data is not evident in the theoretical computation, where instead shows a smooth curve extending from 10 μm to 20 μm. The error bars in figure 6 are computed from the standard deviations of the integrated intensity and average occupancy.

To accommodate a quantitative discussion for length-variation analysis would require that we be able to discriminate clearly between the different fragment sizes in the DNA digest. The λ-mono DNA digest from New England BioLabs contains seven distinct fragment sizes for DNA. We can make histograms of the average occupancy versus contour length and look for areas where the contour length peaks. These peaks should occur at the contour-length values of the fragment sizes in the digest. Figure 7 displays a result of a histogram done for the points of figure 6. For instance, the peak at around *L*≈14.5 μm in figure 7 clearly corresponds to the molecule fragment of length 33,498 base pairs; many of the other fragment lengths can be identified in this way.

With more data points, a Gaussian fit to the binned data can give a better idea of the scatter of each fragment size, and will allow us to better estimate the average occupancy error for various different molecule lengths. To reduce the error in the experiments due to white noise, it is possible to subtract the average background from the image before pixel integration; besides increasing the signal to noise ratio, this further ensures that results from different experiments can be compiled together, without offset due to different experimental conditions.

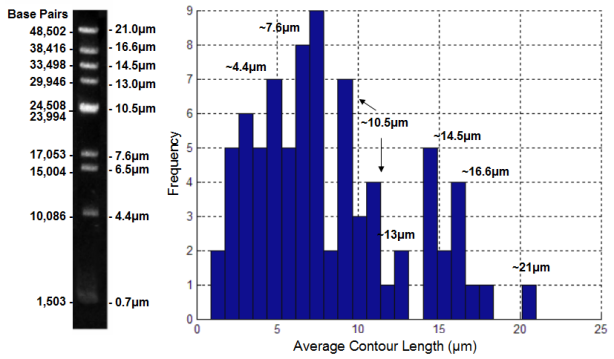

Fig 7. Histogram of the experimental data for the average contour length of a molecule. Peaks distinctly correspond to the fragment sizes observed for the agarose-gel electrophoresis results of a λ-mono DNA digest. Gel-electrophoresis © image reproduced by permission from New England BioLabs.

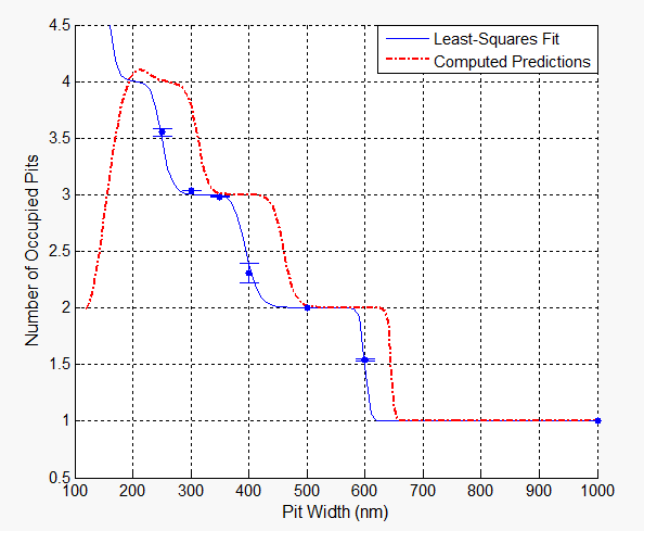

Fig 8. Least-squares-fit of data to theory and comparison to the predicted results obtained from the current definitions of parameters A_o and B_o. Error bars on the data points are the standard error on the averaged mean occupancy for 4, 15, 18, 4, 27, 35 and 21 molecules corresponding to pit widths 250nm, 300nm, 350nm, 400nm, 500nm, 600nm and 1000nm respectively.

C. VARIATION OF PIT WIDTH

An experiment was conducted for L fixed at 21 μm, *h*=*d*=70nm, l=1 μm. A total of 124 molecules were analysed for the average nanopit occupancy with respect to nanopit width. The results were plotted with their associated errors in figure 8. To generate the least-squares-fit curve the following error function was minimized by varying parameters A_o and B_o.

$$\chi = \sum_{a} \left(n_{avg}(A_o, B_o) - n_{exp} \right)^2 \qquad [8]$$

The value of n_{avg} is the numerical result for the mean pit occupancy of a molecule and n_{exp} is the experimentally measured average. In the current theory there are two parameters *A* and *B* which account for the nanopit free energy. The cited scaling (7) of these parameters is

$$A \sim P\left(\frac{1}{h^2} - \frac{1}{(h+d)^2} - \frac{2}{a^2}\right) \quad [9]$$

$$B \sim \frac{w}{(h+d)\ a^2} \quad [10]$$

We have collapsed all the geometric terms except for the pit width variable (*a*) into the parameters A_o and B_o. This results in the following form for *A* and *B*:

$$A \sim P\left(A_o - \frac{2}{a^2}\right) \quad [11a]$$

$$A_o = \frac{1}{h^2} - \frac{1}{(h+d)^2} \quad [11b]$$

$$B \sim \frac{B_o}{a^2} \quad [12a]$$

$$B_o = \frac{w}{(h+d)} \quad [12b]$$

The best fit reveals parameters A_o=102 μm^{-2} and B_o=4.17×10^{-2}. Comparison with the parameters predicted from using equations 11b and 12b with the geometry dimensions for the chip show that the fit parameters A_o and B_o are both smaller by 64.4% than the calculated values. We introduce fitting parameters κ_1 and κ_2 which modify the current predictions for A_o and B_o. Since these experiments were conducted for a different slit height and pit depth than the original experiments by Reisner, κ_1 and κ_2 would be possible functions of these variables. The new fitting parameters would be implemented as follows:

$$A_o = \kappa_1\left(\frac{1}{h^2} - \frac{1}{(h+d)^2}\right) \quad [13a]$$

$$B_o = \kappa_2\left(\frac{w}{(h+d)^2}\right) \quad [13b]$$

A look at the dashed curve in figure 8 obtained from computation using the definitions of parameters A_o and B_o in equations 11b and 12b shows that qualitatively the theory works very well, but it seems to overestimate the average pit occupancy probabilities. However, at *a*=200nm it predicts something very counter-intuitive; the average pit occupancy probability drops drastically. If the nanopit is small compared to the persistence length *P* of the DNA molecule, it may be the case that it is simply energetically unfavourable for the molecule to occupy a nanopit. Introducing the fitting parameters κ_1 and κ_2 can eliminate this abrupt drop in occupancy probability, and seems to show that the excluded volume term (*B*) and the entropic parameter (*A*) exhibit a weaker dependence on slit height and pit depth than currently predicted.

CONCLUSION

We have demonstrated that the theory for predicting the occupancy states for molecule length variation of λ-DNA does not adequately show the sharp transitions that are observed in experiment; pit width variation, however, is in good qualitative agreement. We show that by calibrating the measurements of fluorescence intensity with a known molecule length, it is possible to histogram the average occupancy versus intensity data to discern between variably-sized DNA fragments. We demonstrate that a least-squares fit of the pit-width variation data seems to suggest that the geometric parameters A_o and B_o in current theory may have to be modified. To fit our experimental results to current theory, hypothesized pre-factors, κ_1 and κ_2, were introduced. Future work should be carried out to probe the regimes where counter-intuitive behaviour is predicted by the probability distributions for average pit occupancy (especially where pit widths are below 200nm).

ACKNOWLEDGEMENTS

I wish to thank Prof. Walter Reisner for his generous assistance and guidance throughout this project. Also, I wish thank Qikuan Zhou and André Brandão for their insightful and interesting discussions on how to tackle the lengthy programming for the data analysis, and Alex Klotz for his assistance in conducting the experiments. Finally, I wish to acknowledge NSERC and McGill University for the financial support provided to fund this re search.

REFERENCES

1. P. de Gennes, in *Scaling Concepts in Polymer Physics*. (Cornell Univ. Press, Ithaca, NY, 1979).
2. S. F. Edwards, in *Molcular Fluids*. (Gordon and Breach, London, 1976).
3. C. H. Reccius, John Thomas Mannion, Joshua David Cross, and H. G. Craighead, *Physics Review Letters* **95**, 268101 (2005).
4. W. Reisner *et al. Physics Review Letters* **99**, 058304 (2007).
5. A. Balducci, C.-C. Hsieh, and P. S. Doyle, *Physics Review Letters* **99**, 238102 (2007).
6. E. A. Strychalski, Stephen Levy, and H.G. Craighead, *Macromolecules* **41**, 7716 (2008).
7. W. Reisner, Niels B. Larsen, Henrik Flyvbjerg, Jonas O. Tegenfeldt, and Anders Kristensen, *PNAS* **106**, 79-84 (2009).
8. W. Reisner, *et al. PNAS* **107**, 13294-13299 (2010).
9. D. C. Sullivan, Tiba Aynechi, Vincent A. Voelz, and Irwin D. Kuntz, *Biophysical Journal* **85**, 174-190 (2003).
10 D. Stein, Frank H. J. van der Heyden, Wiepke J. A. Koopmans, and Cees Dekker, *PNAS* **103**, 15853-15858 (2006).
11 S. P. Robert Fisher, Ashley Walker, Erik Wolfart. http://homepages.inf.ed.ac.uk/rbf/HIPR2/log.htm. Accessed July 10th, 2010.

Health and social impacts of geophagy in panama

Lachlan Crawford*[1], Katherine Bodkin[1]

[1]McGill School of Environment, McGill University, 3534 University Street, Montreal, Quebec, Canada H3A 2A7

ABSTRACT

Introduction: Geophagy is a human behaviour involving the ingestion of earthy substances such as soil and clay. Common among pregnant women in rural, tropical areas, it is culturally accepted within some societies and stigmatized within others. There is no scientific consensus on the effects of geophagy on human health. This study was developed as a comprehensive diagnostic to assess the causes, social aspects and potential health impacts of geophagy among pregnant women in rural Panama. **Methods**: Private, structured interviews (n=41) were carried out with women in ten subsistence community farms in the province of Veraguas and the Ngöbe-Bugle Comarca. Additional interviews with healthcare workers were conducted at nearby healthcare facilities. Five soil samples were collected in locations indicated by confirmed geophagists, subjected to simulated human digestion and analyzed for mineral composition and parasite eggs. **Results**: There is no cultural or religious element to the practice; rather it seems to be driven by physiological desires tied to the smell of the material. Prevalence is higher among women with lower education levels and poorer nutritional status suggesting that the practice is associated with low socioeconomic status. Soil analysis did not indicate presence of parasites, but there are potential nutritional benefits of the practice by providing essential minerals missing in the diet. **Discussion**: We find that geophagy in Panama may offer nutritional benefits. However, without a clearer understanding of specific effects of soil in the gastrointestinal tract, it is difficult to determine direct biophysical impacts of geophagy.

KEYWORDS

Geophagy, Health, Pregnancy

*Corresponding author:
lachlan.crawford@mail.mcgill.ca

Received: 2 January 2011
Revised: 5 March 2011

INTRODUCTION

Pica is generally described as the act of habitually eating non-food substances. There is inconsistency in the literature about the precise definition of pica; it has been described as an eating disorder, as an obsessive-compulsive behaviour, or as a normal adaptive response to numerous physiological or environmental conditions *(1-3)*. Geophagy is a type of pica that involves the ingestion of earthy substances such as soil, clay, mud, ash or stones. Humans and animals on almost all continents practice geophagy in a variety of forms, making it one of the most common types of pica *(1, 4, 5)*. In animals, geophagy is considered to be a normal adaptive behavior, that is documented among numerous animal groups including primate species *(6)*. Despite its wide distribution and long documented history, human geophagy is not well

understood. It is acknowledged that the behaviour is most prevalent among populations in tropical climates, and that it is possible to define high-risk groups *(4)*. Populations most likely to engage in geophagy live in rural areas, practice a traditional culture, and have little or no access to modern healthcare facilities *(7,8)*. Within these high-risk communities, geophagy is most common among young children and pregnant women who have a family history of pica, therefore it is perhaps a tradition that is passed on through generations *(8,9)*. Interestingly, geophagy has been shown to be associated with micronutrient deficiencies, especially iron and zinc *(10–14)*. Geophagy has been linked to physiological, cultural, and socioeconomic factors, adding to the complexity and mysterious nature of the behaviour.

BEHAVIOURAL DRIVERS

The many theories developed to explain the etiology of geophagy fall into two main categories: functional and cultural. Functional hypotheses focus on the physiological drivers, whereas the cultural hypotheses focus on the sociological drivers and cultural evolution of earth-eating traditions.

FUNCTIONAL

The first and simplest functional explanation is that people may consume soil or clay because they have insufficient food; incidents of geophagy have certainly been documented in times of famine or food insecurity *(15,16)*. Another functional hypothesis proposes that humans eat earth in response to receiving insufficient nutrients. This crucial link between geophagy and micronutrient deficiencies is supported by the observation that individuals with heightened nutritional needs—children and pregnant women—are the primary geophagists. Some studies propose that it is a pre-existing nutrient deficiency from a lacking diet that creates the physiological desire to engage in geophagy *(12,17,18)*. Others, however, suggest that the ingestion of materials such as clay and soil that binds and blocks the absorption of minerals such as iron and zinc into the bloodstream, thus creating the observed deficiency *(3,8,19,20)*. Soils with high cation exchange capacity (largely negative surfaces) can bind and adsorb nutrient cations to their surface, decreasing their availability for absorption into the bloodstream *(21)*. In simulated human digestion, Hooda et. al. observed a decreased absorption of zinc, iron and copper in solution due to the presence of soil *(21)*. Similarly, Arcasoy et. al. reported a lower iron absorption in iron-deficient children who practiced geophagy when compared to controls *(22)*. A final functional hypothesis incorporates the two viewpoints and suggests that geophagy is both the cause and result of deficiencies. Geophagy may be initially driven by a deficit in the diet but then also leads to the binding of nutrients in the gut, which then exacerbates the deficiencies of the geophagists and reinforces the behavior *(23–26)*. Although many studies have shown a correlation between mineral deficiencies and geophagy, it is difficult to determine the net effect of the ingestion of different soil types on nutrient availability in the gut.

Clay consumption in response to nausea and vomiting is common during early pregnancy, and is evidence that geophagy alleviates gastrointestinal distress. It is postulated that clay and soil can also absorb pathogens and toxins, preventing their entry into the bloodstream or intestinal endothelium *(3,10)*. In fact, kaolin clay was the original active ingredient in Kaopectate, an over-the-counter drug used to treat nausea, vomiting and diarrhea *(10)*. From another theoretical perspective, geophagy is perceived as an adaptive behavior to enhance immune system function. The ingestion of soil may help prevent asthma and aid in the development of a healthy immune system *(9,27)*.

CULTURAL

Eating earth is often associated with rituals, traditions and religion. Hunter suggested that geophagy spread to the Americas during the slave trade, and the activity then disseminated all over North, Central and South America *(1)*. Early reasons for soil eating include supernatural beliefs that soil has the ability to ensure fertility and a healthy pregnancy *(28)*. In many parts of the tropics, earth-eating is a widespread and open practice and is deeply ingrained in traditional culture. It is still common practice to purchase specially prepared clay tablets and other geophagic materials at local marketplaces for consumption in rural areas of the developing world *(4)*. In African societies, geophagy is a social activity that forms part of the feminine identity. It is often carried out collectively in groups of women, but hidden from men of the community *(4, 29)*.

In many parts of Central America, geophagy is clearly deeply ingrained in religious practice. The 'cult of the Black Christ' has resulted in commercially traded white clay tablets available throughout Guatemala, Honduras, El Salvador, Nicaragua and Costa Rica *(1)*. Pilgrimages to holy sites associated with the 'Black Christ' to purchase tablets blessed by the Roman-Catholic Church are made at various times throughout the year *(30)*. Women eat as much as six small tablets of '*tierra santa*' per day hoping to ensure easy pregnancy and childbirth *(1, 30)*.

Note that this strong cultural link is not inherent in all cases of geophagy. In many parts of the world, the practice is highly stigmatized and geophagists carry out the behavior in solitude *(10, 25, 31)*.

CULTURE-NUTRITION HYPOTHESIS

Ultimately, cultural and functional reasons for geophagy are inextricably linked. The high incidence of co-existing geophagy and iron deficiency led to the development of a 'culture-nutrition hypothesis': physiological needs subconsciously determine

behavior, with the behavior often being integrated into cultural practices *(16)*. This proposes that the practice of geophagy is an instinctual behavior, borne out of a biological need for essential minerals, and then incorporated into cultural practices.

Regardless of factors that motivate geophagy, it is still unclear whether the behavior has positive, neutral or negative impacts on human health. The scientific community often defines geophagy as a pathological behavior, an eating disorder, or a symptom of mental illness. This is likely associated with the general acceptance of 'germ theory' which views dirt as a vector for the spread of disease *(32)*.

HEALTH IMPACTS

The best-studied potential consequence of geophagy is the risk of ingesting soil-borne infectious parasites. Two organisms that are of concern during pregnancy are hookworm and *Toxoplasma gonii*, associated respectively with malnutrition and fetal nervous system damage *(2, 33)*. Another proposed consequence of geophagy is lead poisoning, with numerous reported case studies suggesting the co-occurrence of lead poisoning and geophagy *(34-36)*. Lead exposure can lead to maternal and fetal kidney damage, encephalopathy and impaired cognitive function *(35)*. Other documented health impacts include constipation, bowel obstruction, hypokalemia, poisoning due to other toxins present in the environment and a possible exacerbation of malnutrition *(35)*. Additionally, some studies have hypothesized possible associations of maternal geophagic behaviour with negative birth outcomes such as low birth weight, neural tube defects, small head circumference, premature birth, and elevated perinatal mortality, likely due to heavy metal toxicity and maternal malnutrition *(25,37)*. Finally, others have concluded there is no specific pregnancy outcome associated with geophagy *(38,39)*.

Many studies have treated geophagy as a behaviour that may provide nutrients otherwise absent in the diet *(10)*. The types of soil most commonly consumed tend to be high in calcium or iron *(11)*. Studies comparing the micro-nutritional value of geophagic material and pharmaceutical supplements for pregnancy show surprising comparability for several important nutrients including calcium, magnesium and iron *(25)*. Although the extent of soil absorption in the intestinal tract is unknown, it is possible that geophagists receive nutrients from the soil. Thus, there are potential benefits of geophagy that cannot be discounted, and must be explored to understand the implications of this behavior.

The practice of human geophagy, particularly during pregnancy, clearly has substantial and pertinent implications for maternal and child health as well as effects on social interaction and behaviour patterns in poor, rural communities. Studying the prevalence and impacts of this behaviour is becoming increasingly important, as the growing widespread use of agrochemicals in Panamanian agriculture *(40)* is causing high levels of toxic chemicals in soils that may be ingested. This study was developed to assess the causes as well as the social and biophysical impacts of human geophagy during pregnancy in Panama in order to understand its general context in a country where it has not previously been documented. Components of the study included informal interaction and observation within rural communities, structured individual interviews, and analysis of soil composition of confirmed geophagic materials.

Fig 1. Map of Panama showing provincial boundaries
Image used under creative commons license; accessed from http://mapsof.net/uploads/static-maps/countries_panama_provinces_2005_10_18_en.png

Fig 2. Map of Veraguas, Panama (green circles demark farms visited.)
Image used under creative commons license; accessed from http://mapsof.net/panama/static-maps/jpg/veraguas-panama-political-map

METHODOLOGY

Data were collected at 10 community-owned farms in western Panama, in the province of Veraguas and the *Ngöbe-Buglé comarca* land reserve (Fig. 1). Access to the farms was provided through the local NGO the '*Patronato de Nutrición*' that works with rural subsistence farmers to manage and run community farms. For the purposes of this project, farms were selected based on accessibility (Fig. 2). Data collection began with a concise, neutral introduction to geophagy including a description of the behaviour and summaries of both possible benefits and risks to maternal and child health, combined with an explanation of the research project and objectives. The introduction was given to all members of a farm and time was allowed for public sharing of stories or opinions on the topic by members of the community. This was followed by obtaining informed consent and conducting private, structured interviews with female volunteers (n=41) from the group using a questionnaire and interview methodology written in accordance with the McGill University Protocol for Research in Panama's Indigenous Communities *(41)*. Additional interviews were conducted with health care workers at the regional Hospital Ezequiel Abadía in Soná, Veraguas, and at the health center at Nuestra Señora del Camino in San Félix, Chiriquí. Five samples of approximately 100g of geophagic material, identified by confirmed geophagists were collected. Laboratory analysis for parasite eggs was carried out by the Parasitology Department of the University of Panama using a 3-step process of simple sedimentation, and treatment with formolether, and flotation. Mineral composition of the samples was determined by the "*Instituto de Investigaciones Científicas y Servicios de Alta Tecnología*" (INDICASAT) following the methodology in Geissler et. al. *(42)*: from each sample, 10.0g were shaken with 100ml of 0.1M HCl for 2 hours to simulate human digestion and the filtrate was examined for select minerals by inductively coupled plasma (ICP) mass spectrophotometry *(42)*.

RESULTS

The prevalence of confirmed geophagy among women interviewed was 22.5%. The most commonly consumed materials were red non-porous clay, red dry soil and yellow dry soil, with more infrequent reports of termite mound soil, river rocks and wet ash. Although some women practiced geophagy throughout their lives, it was most common during childhood and pregnancy. The average amount consumed was shown as handfuls by geophagists and approximated as 50g per event, ingested about once a week. Discussions revealed a strong stigma associated with the behaviour: almost all geophagists practiced in complete solitude and expressed embarrassment in response to their actions. Those that admitted to a desire to partake in geophagy without having done so (12.2%) explained that they did not do so because the staff at the local *Centro de Salud* (health centre) told them it was dangerous. As well, geophagists reported an intense desire to ingest the material associated with its smell, and an increased likelihood of engaging in geophagy after heavy rainfall. Overall, confirmed geophagists had more children, lower estimated infant survival (calculated by dividing the number of children to survive past age 5 by the total number of births in the mother's lifetime), were older in age, ate animal protein less frequently and had fewer years of formal education than non-geophagists (*Table 1*).

Interviews with health care workers in the regional urban government hospital in Soná and rural non-government health center in San Félix revealed a perception that geophagy is an unhealthy vice that should be discouraged. The head nurse of obstetrics in the regional hospital believed geophagy used to be more common but is now almost unheard of due to the improvement of access to healthcare in Panama since the 1980s. Conversely, the worker at the small health center maintained it was very common in rural and indigenous areas and is recognized as one of the first symptoms of pregnancy. Both health care workers believed geophagy could lead to premature birth, maternal and fetal malnutrition and peri-natal complications.

Laboratory analysis of geophagic material samples revealed that no sample contained any human parasite eggs or any detectable amounts of lead or nickel; however they did contain considerable amounts of essential minerals such as copper, iron and magnesium.

	Geophagic women (n=9)	**Geophagic women** (n=9)	**p-value**
Average Age (years)	47.9	40.3	0.194 *(2-tailed t-test)*
Average # Children	6.1	4.8	0.271 *(2-tailed t-test)*
Estimated Infant Survival Rate	88.7%	93.9%	0.18 *(chi-square)*
Meat > 1/Week	0%	39.4%	0.054 *(chi-square)*
Literacy Rate	55.6%	96.9%	0.001 *(chi-square)*
Average # yrs of education	3.2	5.6	0.009 *(2-tailed t-test)*

Table 1. Comparison of pertinent socioeconomic indicators that were evaluated among interviewees

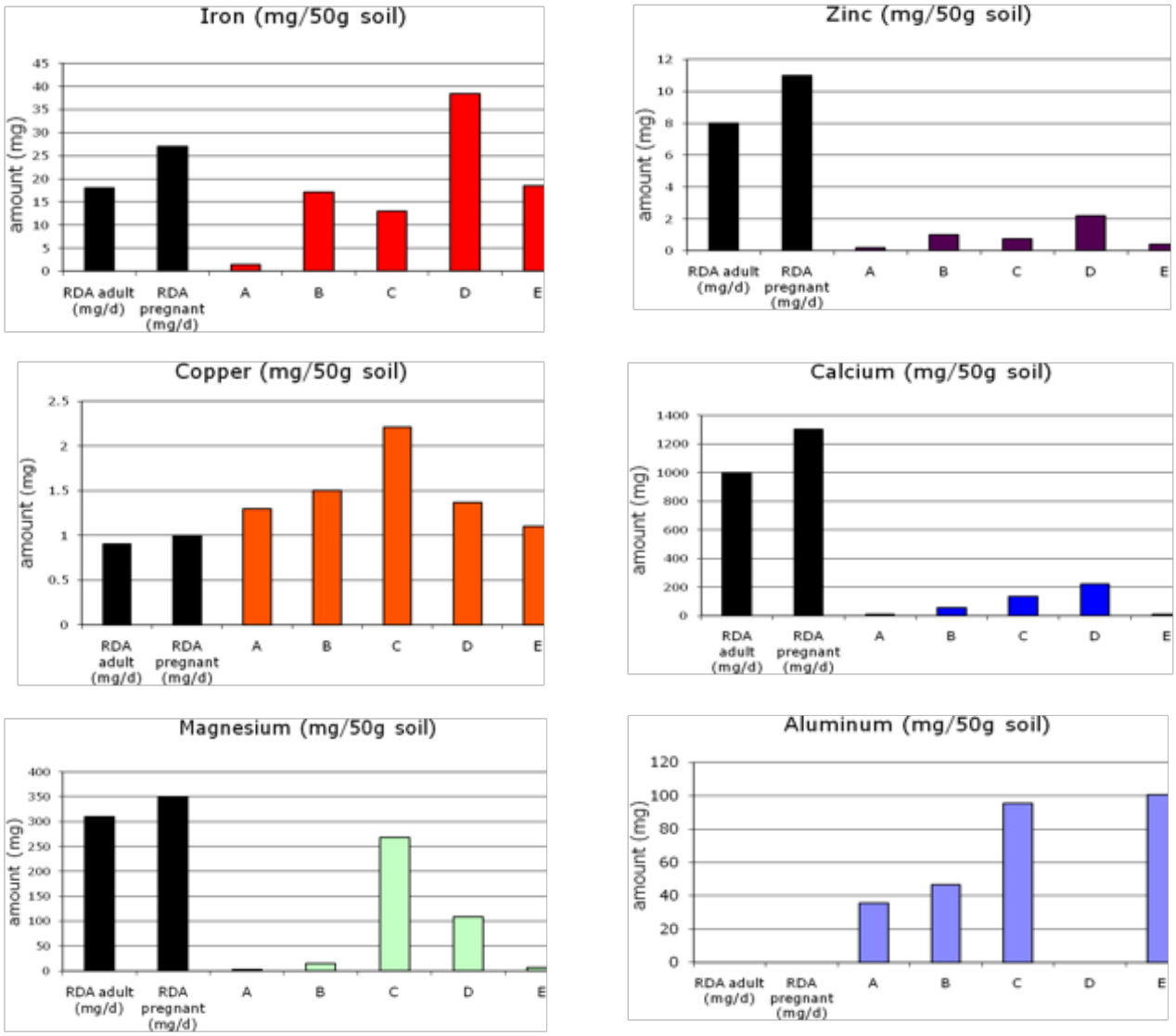

Fig. 3 Nutrients in soil available for absorption in an average single geophagic event of 50g soil. Amounts of the five soil samples are compared to Health Canada's recommended daily allowances (RDAs) (43, 44) for adults (first column) and for pregnant women (second column) for six nutrients. No sample had any detectable amounts of lead or nickel

DISCUSSION

This is the first documented study of geophagy in Panama. In the examined area, there is no apparent cultural or religious component to the behaviour. All confirmed geophagists indicated that they carried out the activity in solitude in response to a strong desire for the material associated with its smell. For many of the respondents, the formal interview was the first time they had spoken about geophagy. Because of the strong stigma associated with the behaviour, it is extremely likely that the prevalence of geophagy is higher than observed, thus making analysis of associated socioeconomic and health effects extremely difficult.

The observed social stigma associated with geophagy is clearly perpetuated by local health care workers that regard it as an undesirable act. Some of the interviewees expressed a desire to engage in geophagy but had never done it because they were given the impression by healthcare workers that it was a dangerous and unhealthy practice. However, if geophagy is an adaptive response to a physiological need, it is entirely possible there are nutritional benefits gleaned by those who desire to engage in this activity. Until we have a more full understanding of its impacts on health and social interaction within a community, the subject should be approached with neutrality and sensitivity by both researchers and health care workers.

One notable observation was the correlation between socioeconomic factors and geophagy. There was a strong, statistically significant association between levels of education and geophagy, with geophagic women reporting fewer years of education ($p=0.009$) and lower literacy rates ($p=0.001$). This is interesting because it points to geophagy being more strongly linked with education as opposed to nutrition. Statistically insignificant associations include less meat intake ($p=0.054$), lower infant survival rate ($p=0.18$), older age ($p=0.194$) and greater number of children ($p=0.271$). An increase in sample size is required in order to guarantee statistical significance of results and run regression modeling in order to determine relative strength of correlation. In agreement with previous studies linking the behaviour with iron deficiency and anemia, we found geophagy to be more common in individuals with lower frequency of meat consumption and poorer overall nutrition in general. Many of the geophagic women indicated they did not have enough food for three meals a day, and were subsisting on rice and beans, with meat consumption occurring less than once per week. The iron, copper and magnesium from a 50-g sample of the soil could potentially contribute substantially to meeting Health Canada's recommended daily allowances for essential micronutrients (*Fig. 3*).

If the behaviour is in fact driven by iron-deficiency anemia or other micronutrient deficiencies, geophagy may be a physiologically corrective behaviour. However, in vitro attempts by Hooda et. al (2004) to determine actual benefit from samples of geophagic materials suggest a net decrease in nutrient absorption for iron, copper and zinc, despite the minerals being present in the soil itself *(21)*. Conversely, the study also suggests the same soils may increase the absorption of other nutrients such as calcium, magnesium and manganese, yet this varies for different samples studied. Clearly, the mechanisms of nutrient absorption are complex across different soils and for different minerals. In our study, we observed a large contribution of the daily requirement of iron and other minerals by the soil after a simple simulated human digestion. Yet it is clear that without a complete and in-depth absorption analysis like that done by Hooda et. al. for these specific samples, it is difficult to draw final conclusions on the overall physiological benefits or harm of the observed geophagy.

In three communities, there were reports of people having severe medical complications due to geophagy. There were reported incidences of abdominal swelling, yellowing of the skin, and death due to soil consumption. However, there were no available hospital records to confirm this. Yellow skin and abdominal swelling are both symptoms of liver failure, which may indicate parasite infection or heavy metal poisoning *(45)*. Although we found no evidence of human parasite eggs, our limited sample size made it unlikely that we would detect such parasites. None of the soil samples had any detectable levels of lead or nickel. Copper intake from 50g soil is below the acute copper toxicity limit of 15mg/d *(43)*. Aluminum intake from 50g of any of the soil samples was well below the acutely dangerous level of 302mg of aluminum/day *(46)*, but the accumulation of aluminum in the body over time even at lower levels of intake per day may negatively affect blood iron levels and nerve function *(46)*. Adverse effects of geophagy indicative of liver failure, such as those reported in the farms, could occur if the amount of soil ingested exceeds approximately 150-200g per day, an amount substantially higher than the average 50g per week.

CONCLUSION

In this study, we show that geophagy exists in modern day Panama among the rural poor. Women carry out this highly stigmatized behavior in private, primarily during pregnancy and childhood. Soil samples of confirmed geophagic materials indicate no presence of parasites or acutely dangerous levels of heavy metals, and the potential for nutritional benefits. Within rural communities, geophagy was most notably linked to lower levels of education, and may be linked to poorer nutritional status, more children, and older age. The multifaceted nature of this topic of research calls for an interdisciplinary team of researchers in order to effectively evaluate its prevalence and potential health impacts. Further studies are needed to investigate the physiological impact of soil ingestion on mineral status, to increase the sample size, and delve into causative pathways and health outcomes of this under-studied behaviour in rural Panama.

ACKNOWLEDGEMENTS

First and foremost, we will forever be indebted to the people of the farms: Limón, Calabaso, La Grama, Cabuya, Jacinto, Barrigón, Cocuyal, Rincón Grande, Torontún and Peña Blanca. They exceeded our expectations for the field component of this project with their generosity, openness and acceptance.

Furthermore, we are extremely grateful to the Patronato de Nutrición. Despite the fact that there was no prior evidence of geophagy in Panama, they gave us every opportunity to explore this topic and provided us with the necessary resources for our interviews and data collection. In particular, we would like to thank Eric Gonzalez and Danya Amores, for their patience, dedication and enthusiasm.

We would also like to thank Albano Diaz at INDICASAT laboratory, Rigoberto Fernandez and Nilia Morales from the Department of Parasitology at the University of Panama, Sra. Juana at

the Hospital Ezequiel Abadía de Soná, Veronica Gall from the 'Fundación Nuestra Señora del Camino', Dr. Sera Young and Dr. PW Geissler for their correspondence and advice, our supervisors Dr. Marilyn Scott and Dr. Kristine Koski, Rafael Samudio, Roberto Ibañéz, and Carlos Arias Mejia for their academic guidance and support throughout this project, McGill University, and The Smithsonian Tropical Research Institute.

REFERENCES

1. J.M. Hunter, R.D. Kleine, *Geogr. Rev*. **74**, 157-169 (1984).
2. P.W. Abraham, in *Soil and Culture*, E.R. Landa and C. Feller, Eds. (Springer Netherlands, 2009), p.p. 369-398.
3. T. Johns, M. Duquette, *Am. J. Clin. Nutr*. **53**, 448-456 (1991).
4. P.W. Abraham, J.A. Parsons, *Geogr. J*. **162**, 63-72 (1996).
5. P.W. Geissler, D. Mwaniki, F. Thiong'o, H. Friis, *Trop. Med. Int. Health*. **2**, 624-630 (1997).
6. R. Krishnamani, W.C. Mahaney. *Anim. Behav*. **59**, 899-915 (2002).
7. R.W. Corbett, C. Ryan, S.P. Weinrich, *Am. J. Matern. Child. Nurs*. **28**, 183-188 (2003).
8. R.D. Horner, C.J. Lackey, K. Kolasa, K. Warren, *J. Am. Diet. Assoc*. **91**, 34-39 (1991).
9. G.N. Callahan, *Emerg. Infect. Dis*. **9**, 1016-1021 (2003).
10. S.L. Young, M.J. Wilson, D. Miller, S. Hillier. *PLoS ONE*. **3**, e3147 (2008).
11. A.S. Wiley, S.H. Katz. *Cur. Anthropol*. **39**, 532-545 (1998).
12. S. Singhi, R. Ravishanker, P. Singhi, R. Nath. *Indian. J. Pediatr*. **70**, 139-143 (2003).
13. C. Beyan, K. Kaptan, A. Ifran, E. Beyan. *Arch. Med. Sci*. **5**, 471-474 (2009).
14. J.R. Alice, *J. Am. Diet. Assoc*. **98**, 293-296 (1998).
15. J. Castro, J. Boyd-Orr. *The Geography of Hunger* (Little Brown and Company, Boston, 1952).
16. J.M. Hunter, *Geogr. Rev*. **63**, 173-195 (1973).
17. B. Von Bonsdorff, *Brit. J. Haemat*. **35**, 476-477 (1977).
18. R. Kushner, V. Shanta Retelny, *Obes. Surg*. **15**, 1491-1495 (2005).
19. P.W. Geissler, *Africa*. **70**, 653-682 (2000).
20. P.S. Hooda, C.J.K. Henry, T.A. Seyoum, L.D.M. Armstrong, M.B. Fowler, *Environ. Geochem. Health*. **24**, 305-19 (2002).
21. P.S. Hooda, C.J.K. Henry, T.A. Seyoum, L.D.M. Armstrong, M.B. Fowler. *Sci. Total. Environ*. **333**, 75-87 (2004).
22. A. Arcasoy, A. Cavdar, E. Babacan. *Acta Haemat*. **60**, 76-84 (1978).
23. C. Brand, L.D. Jager, G-I. Ekosse. *J. Med. Technol*. **23**, 11-3 (2009).
24. Nchito, Mbiko, Geissler, Wenzel P, Mubila, Likezo, *et al.* (Elsevier, Kidlington, UK, 2004).
25. L.B. Lopez, C.R.O. Soler, M.L.P.M. de Portela. *Arch. Latinoam. Nutr*. **54**, 3 (2004).
26. E. Lacey, *Public. Health. Rep*. **105**, 29-35 (1990).
27. S.T. Weiss, *New Engl. J. Med*. **347**, 930-931 (2002).
28. M. Gelfand, *East. Afr. Med. J*. **22**, 98-103 (1945).
29. D.E. Vermeer, *Ann. Assoc. Amer. Geogr*. **56**, 197-204 (1966).
30. Borhegyi S. *El Palacio*. **61**, 387-401 (1954).
31. D.E. Vermeer, *Ann. Assoc. Amer. Geogr*. **65**, 414-24 (1979).
32. J. Henry, A.M. Kwong, *Deviant Behav*. **24**, 353-71(2003).
33. A.I. Luoba, P.W. Geissler, G. Estambale, J. Ho, D. Alusala, R. Ayah, *Trop. Med. Int. Health*. **10**, 220-227 (2005).
34. B. Hackley, A. Katz-Jacobson, *J. Midwifery. Womens. Health*. **48**, 30-38 (2003).
35. M. Mills, *Nursing for Women's Health*. **11**, 266-273 (2007).
36. G. Erdem, X. Hernandez, M. Kyono, C. Chan-Nishina, L. Klwaishi, *Clin. Pediatr*. **43**,185-188 (2004).
37. S.L. Carmichael, G.M. Shaw, D.M. Schaffer, C. Laurent, S. Selvin, *Am. J. Epidemiol.* **158**, 1127-1131 (2003).
38. R.W. Corbett, C. Ryan, S.P. Weinrich. *Am. J. Matern. Child. Nurs*. **28**, 183-188 (2008).
39. A.J. Rainville, *J. Am. Diet. Assoc*. **98**, 293-296 (1998).
40. C.I. Nicholls, M.A. Altieri. *Int. J. Sust. Dev. World.* **4**, 93-111 (1997).
41. R. Cansarí, Y. Cárdenas, A. Chiari, H. López, E. Lucas, F. Johnson, et al. Protocol for Research in Panama's Indigenous Communities. *Protocols and ethics in the Aboriginal Environment* [serial on the Internet]. 2006: Available from: http://www.mcgill.ca/files/pfss/protocol.pdf.
42. P.W. Geissler, C.E. Shulman, R.J. Prince, W. Mutemi, C. Mnazi, H. Friss, *et al. T. Roy. Soc. Trop. Med. H*. **92**, 549-53 (1998).
43. Health Canada. *Dietary Reference Intakes for Vitmain A, Vitamin K, Arsenic, Boron, Chromium, Copper, Iodine, Iron, Manganese, Molybdenum, Nickel, Silicon, Vanadium and Zinc* (2001).
44. Health Canada. *Dietary Reference Intakes for Calcium, Phosphorus, Magnesium, Vitamin D, and Fluoride*. (1997).
45. D.L. Longo, A.S. Fauci, Eds. *Harrison's Gastroenterology and Hepatology.* (McGraw-Hill, Bembo, 2010).
46. Health Canada. *Aluminum [Technical Document - Chemical/Physical Parameters]*. (1998).

Role of Dscam mediated self-avoidance and tiling in neural branching

Marzieh Ghiasi*[1]

[1]Department of Anatomy and Cell Biology, McGill University, Strathcona Anatomy & Dentistry Building, 3640 University Street, Montreal, Quebec, Canada H3A 2B2

ABSTRACT

Dscams (Down syndrome cell adhesion molecules) play an important role in the formation of neural circuits. Various studies have highlighted the role of Dscams in two major wiring strategies, self-avoidance and tiling, leading to broad and uniform branching. The *Drosophila* Dscam1 protein, which has thousands of isoforms formed by alternative splicing, has been shown to confer unique identities to cells and mediate homotypic recognition, homophilic repulsion and consequently self-avoidance behavior between neurites of a single neuron. The *Drosophila* Dscam2 protein mediates homophilic repulsion between projections from the same class of cells, in a process called tiling. The vertebrate Dscam has been shown to mediate both tiling and self-avoidance. However, the mechanisms by which this is accomplished in the absence of homotypic recognition are unclear. This review provides an overview of functional similarities and differences between Dscam homologues in invertebrate and vertebrate species, and describes some mechanisms proposed to account for these differences.

KEYWORDS

Self-avoidance, tiling, neural circuitry, Down syndrome

*Corresponding author:
marzieh.ghiasi@mail.mcgill.ca

Received: 2 January 2011
Revised: 8 March 2011

INTRODUCTION

The formation of neural circuitry occurs under the direction of many molecules that guide axons to form proper synapses. Dscam (Down syndrome cell adhesion molecule), a cell surface protein first identified by Yamakawa *et al.*, belongs to a class of the immunoglobulin (Ig) family of molecules. Dscam in particular is involved in recognition processes between neurons and plays an essential role in mediating the formation of extensive and complex connections in the brain. The human *Dscam* gene was isolated from the chromosome band 21q22.2-22.3, a region implicated in many neurological phenotypes observed in Down syndrome *(1)*. The invertebrate *Dscam* gene, a homologue of the vertebrate Dscam, was isolated by Schmucker *et al.* in *Drosophila melanogaster* (fruit fly) *(2)*. The Dscam protein has been implicated in a variety of functions in different species. It confers unique identities to cells in fruit flies *(3)* and mediates dendritic and axonal synaptic targeting in fruit flies, chicks and mice *(4)*, as well as synaptogenesis in *Aplysia* (sea slug) *(5)*. Dscam's role in innate immunity in flies is under investigation (6).

While the vertebrate *Dscam* gene appears to have shared a common ancestor with the invertebrate *Dscam*, they have very different functional characteristics. Drosophila, in particular, has four classes of *Dscam* genes (*Dscam 1–4*). The *Dscam1* gene has 24 exons, and four of these exons (4, 6, 9, 17) contain cassettes of genes that undergo mutually exclusive alternative splicing *(7)*. Exon six, for instance, has forty-eight variants within its array, but only one of these variants will contribute to the mature transcript. This form of alternative splicing in the fly *Dscam1* produces as many as 38,016 unique isoforms of the protein. This trait is not shared by other *Dscam* classes in flies or by the vertebrate *Dscam (2, 7)*. Nonetheless, all *Dscams* have conserved molecular functions required for neural wiring. These "core molecular mechanisms" *(8)* allow for self-avoidance and tiling leading to generation of structured axonal and dendritic pathways.

REVIEW

Self-avoidance allows the axons and dendrites extending from a single neuron to repel one another, thereby branching widely and uniformly covering the synaptic field. Tiling allows neurites, axonal and dendritic projections, of different cells of the same functional class to repel one another, thereby preventing overlapping of synaptic domains *(9)*. In this review I examine how Dscam is involved in these mechanisms that allow for neural branching.

Kramer and Stent *(10)* first characterized self-avoidance in neurons in a study of the giant Amazon leech, *Haementeria ghilianii*. They found that branches from different neurons innervating the organism overlapped, whereas branches rising from the same neuron did not overlap. To account for this observation, Kramer and Stent proposed that molecular cues conferred unique identities to neurons and allowed for homotypic recognition, that is recognition that they possess the same identity *(10)*. Self-avoidance has been observed as a universal mechanism in neuronal branching *(9)*.

Tiling of neurons was first characterized by Wassle *et al. (11)* in retinal ganglion cells (RGCs) of cats. They found that ganglion cells consisted of subpopulations whose dendritic field size—the breadth of the area with which dendrites extending from the cell interact—was limited by interactions with neighboring cells of the same class. This finding was corroborated in rat RGCs by Perry and Linden *(12)*, who identified different classes of RGCs and found that if an area in the developing rat retina was depleted of a class of RGCs, neighboring cells of the same class extended dendrites into the area, recovering a uniform dendritic receptive field.

HOMOTYPIC RECOGNITION, HOMOPHILIC REPULSION AND SELF-AVOIDANCE MEDIATED BY DSCAM1

Dscams are thought to guide neuronal branching largely via homophilic repulsion, a process in which after some recognition event molecules of the same type repel one another. Of the four classes of Dscams in *Drosophila*, Dscam1 mediates self-avoidance while Dscam2 mediates tiling, both via homophilic repulsion *(13)*. In vertebrates, only two Dscam molecules exist (DSCAM and DSCAML1). These have been observed to mediate both self-avoidance and tiling. The exact mechanism is currently the subject of debate *(14)*.

Evidence for homophilic repulsion leading to self-avoidance was shown by Matthews *et al. (15)*. They observed that in neurites extending from the same neuron, after contact and homotypic recognition the neurites withdrew and segregated in a manner consistent with homophilic repulsion. They postulated that homophilic repulsion is mediated by the ability of *Drosophila* Dscam molecules to confer unique identities to cells by generating of thousands of isoforms. Possessing the same isoforms allows neurites to recognize other neurites extending from the same cell. Studies have found that inducing the expression of the same *Dscam1* isoforms in different classes of cells leads to self-avoidance between these cells (16). Examining an olfactory ganglion called the mushroom body in the *Drosophila* brain, Zhan *et al. (17)* concluded that the composition of the isoform is not important in establishing circuitry; rather, the difference between the isoforms—the diversity—is critical.

As an additional safeguard to prevent binding between similar proteins, Dscam1 has "all-or-none" structural and biochemical binding properties. The homophilic binding region of Dscam1 is composed of eight immunoglobulin (Ig) domains. Three of these domains, making up about 80% of the region, are highly variable because of alternative splicing of the gene as described earlier. All these variable protein domains must match in order for binding between isoforms to occur creating an S-shaped homodimer *(18)*. This configuration of Dscam1 ensures that isoforms with slight variations neither bind nor homotypically recognize one another.

TILING AND SELF-AVOIDANCE MEDIATED BY DSCAM HOMOLOGUES

The contribution of other Dscam class members is critical to the formation of neural circuitry. The *Drosophila* Dscam2 presents a framework for understanding vertebrate Dscam function, as neither undergoes the extensive alternative splicing of Dscam1. Furthermore, while the majority of neurons in *Drosophila* express Dscam1, Dscam2 expression is limited and cell-type specific, as is Dscam expression in vertebrates *(9)*.

In flies, Dscam2 is thought to be involved in allowing projections from different cells of the same functional classes to avoid each other, otherwise known as a process called tiling *(15)*. Millard *et al. (13)* examined lamina (L1) neurons in the *Drosophila* retina which receive input from eye photoreceptors. L1 neurons normally form highly discrete vertical columns. Mutant L1 neurites lacking Dscam2 were shown to laterally invade adjacent neighboring columns and were no longer able to properly tile *(13)*.

Vertebrate Dscams have been found to regulate both self-avoidance and tiling. Loss-of-function experiments in DSCAM-expressing mouse amacrine cells, whose dendrites are normally evenly spaced in the internal plexiform layer (IPL) of the retina, led to fasciculation dendrites from different cells of the same class *(19)*. This is consistent with the process of tiling described by Wassle *et al.* in cat retinas *(11)*. The study also found that without properly functioning DSCAM, processes extending from the same amacrine neurons which normally did not overlap with one another now overlapped *(19)*. This indicates that the vertebrate Dscam is also involved in self-avoidance.

Given the preservation of core functional mechanisms of the fly Dscam1 in vertebrate Dscams, it is perplexing that vertebrate Dscams lack the isoform diversity considered critical to the neuronal self-avoidance mechanism in *Drosophila*. Although it is clear that vertebrate Dscams mediate self-avoidance; they do not appear to confer unique identities to neurites *(8)*. The mechanisms by which vertebrate Dscams function without homotypic recognition is unclear *(19)*.

Although structurally vertebrate Dscams are homophilic adhesion molecules, congruent with *Drosophila* Dscams, certain functional incongruities between these have led to speculation about the possibility of alternative pathways mediating self-avoidance. One hypothesis described by Fuerst *et al.* suggests that vertebrate Dscams act via passive repulsion; that is , they act as a "non-stick coating" *(14)* in a small subset of cell masking these cells' intrinsic adhesion properties. Establishing such "exclusion zones" around cells would negate the need for molecular diversity and, by extension, homotypic recognition.

Given that the *Drosophila* Dscam and vertebrate Dscam proteins share the same structure and general binding properties, it is possible that the evolution of other recognition systems may have provided vertebrates with a different strategy for homotypic recognition than that of invertebrates. This recognition system may under the guidance of Dscam co-receptors that, during vertebrate evolution, took over the functional role of isoform specificity seen in invertebrate Dscam *(8)*. The existence and function of such co-receptors has yet to be confirmed.

PERSPECTIVES

Dscam in vertebrates and its arthropod homologue Dscam have been implicated in mediating self-avoidance and tiling via homophilic interactions. Alternative splicing of Dscam1 confers unique identities to neurons, which is used for homotypic recognition, binding and homophilic repulsion between axons and dendrites extending from these neurons. Dscam2, though not alternatively spliced to the extent of Dscam1, also uses homophilic repulsion to mediate tiling. However, the mechanisms by which vertebrate Dscam guide development have yet to be delineated. Studies elucidating self-recognition mechanisms in vertebrate neurons and different intracellular pathways that Dscam molecules can activate will lead to greater understanding of the formation and development of neural circuitry.

REFERENCES

1. K. Yamakawa *et al., Hum. Mol. Genet*. **7**, 227 (February 1, 1998).
2. D. Schmucker *et al., Cell* **101**, 671 (2000).
3. D. Schmucker, *Nat Rev Neurosci* **8**, 915 (2007).
4. D. Hattori *et al., Annual Review of Cell and Developmental Biology* **24**, 597 (2008).
5. H.-L. Li *et al., Neuron* **61**, 527 (2009).
6. F. L. Watson *et al., Science* **309**, 1874 (September 16, 2005).
7. W. M. Wojtowicz *et al., Cell* **118**, 619 (2004).
8. D. Schmucker, B. Chen, *Genes & Development* **23**, 147 (January 15, 2009).
9. S. S. Millard, S. L. Zipursky, *Current Opinion in Neurobiology* **18**, 84 (2008).
10. A. Kramer, G. Stent, *J. Neurosci.* **5**, 768 (March 1, 1985).
11. H. Wassle, L. Peichl, B. B. Boycott, *Nature* **292**, 344 (1981).
12. V. H. Perry *et al., Nature* **297**, 683 (1982).
13. S. S. Millard, *et al., Nature* **447**, 720 (2007).
14. P. G. Fuerst *et al., Neuron* **64**, 484 (2009).
15. B. J. Matthews *et al., Cell* **129**, 593 (2007).
16. M. E. Hughes *et al., Neuron* **54**, 417 (2007).
17. X.-L. Zhan *et al., Neuron* **43**, 673 (2004).
18. M. R. Sawaya *et al., Cell* **134**, 1007 (2008).
19. P. G. Fuerst *et al., Nature* **451**, 470 (2008).

Challenges and solutions to the worldwide tuberculosis epidemic

Ben Landon*[1]

[1]McGill Department of Physics, McGill University, Ernest Rutherford Physics Building, 3600 rue University, Montreal, Quebec, Canada H3A 2T8

ABSTRACT

Tuberculosis is an infectious bacterial disease responsible for a current worldwide epidemic which results in 1.5 million deaths per year. Citizens of developing countries, especially in Africa and Asia, are at a higher risk of infection and death. In some developing countries, as much as 80% of the population tests positive for latent tuberculosis infection, in comparison to approximately 5% for developed countries such as the United States. Studies of the current vaccine Bacillus Calmette-Guerin show that elicits a decreased immune response in patients from some areas of the world. In treating tuberculosis, the World Health Organization has developed DOTS, Directly Observed Treatment, Short course, a program which has evolved from a simple treatment regiment to a complete guideline on political involvement, logistics and medical operations and has been met with astounding success rates. New diagnostic techniques and vaccines currently in research bring promise to combatting and ending the tuberculosis epidemic.

KEYWORDS

Tuberculosis, DOTS, MVA85A, Bacillus Calmette Guerin

*Corresponding author:
benjamin.landon@mail.mcgill.ca

Received: 3 January 2011
Revised: 8 March 2011

INTRODUCTION

Tuberculosis (TB) is an infectious bacterial disease that results in over 1.5 million lives every year. 75% of TB cases cause lesions in the lungs which can spread to other parts of the body *(1)*. The World Health Organization declared tuberculosis an epidemic in 1993 *(2)*. In developing countries, poor standards of medical care lead to misdiagnosis and mistreatment of the disease and result in a high number of tuberculosis-related deaths, as well as the development of drug resistant strains of the bacteria. Environmental conditions lead to decreased efficacy of the only existing tuberculosis vaccine, *Bacilius Calmette-Guerin* (BCG). Coinfection of HIV and TB have also resulted in especially high mortality rates in certain parts of the world, especially Sub-Saharan Africa *(3)*.

The bacterium responsible for TB, *Mycobacterium tuberculosis*, is primarily spread by the coughing and sneezing of individuals in whom the disease has become active. Infection begins when the mycobacteria reach the lungs and begin to replicate, forming the primary tuberculosis lesion, termed a "Ghon focus". Secondary lesions often form in other areas of the lungs and can form anywhere in the body once the bacteria enter the bloodstream *(4)*.

A distinction should be made between active and latent tuberculosis. The active tuberculosis disease is responsible for the deaths and symptoms and is the treatable form of the disease. However, humans can still carry the bacteria without showing symptoms and can spread it through coughing and sneezing – this is known as latent tuberculosis infection (LTBI).

GEOGRAPHICAL DISPARITY & VACCINE EFFICACY

Incidence of tuberculosis is not uniformly spread throughout the globe. Citizens of developing countries, especially in Africa and Asia, are at a higher risk of infection and death. In some developing countries, as much as 80% of the population tests positive for LTBI, in comparison to approximately 5% for developed countries such as the United States. TB mortality is more than ten times higher in Africa than in North and South America *(5)*.

Currently, the only vaccine available for tuberculosis is *Bacilius Calmette-Guerin* (BCG). Although vaccination rates are high in some areas where tuberculosis is endemic, data has suggested that vaccine efficacy may vary by geographical location. In general, BCG produces about 60-80% protection in individuals when administered in North America, while clinical studies in tropical climates usually show that the vaccine has little to no effect.

Reasons for variable efficacy of the vaccine are currently not fully understood. Suggested hypotheses include variation in the strain of the vaccine, genetic variation in the vaccinated population, and variable background exposure to tuberculosis bacteria and the vaccine strain itself. There is evidence suggesting that the vaccine efficacy diminishes in tropical regions because the vaccinated population experiences more background exposure to mycobacteria than the populations of non-tropical regions. A study published in 2002 suggested a negative correlation between existing mycobacterial resistance and vaccine effectiveness. The study tested schoolchildren from Malawi and the UK by administering an interferon-gamma response test and a tuberculin protein skin response test, testing for vaccine response. The results suggest that because the Malawian children had an existing immunity to mycobacteria, the introduction of the BCG vaccine (also a mycobacteria) produced no change in their immune systems. In contrast, the British schoolchildren, with no previously existing bacterial immunity, developed mycobacterial resistance from the BCG vaccine *(6)*.

TREATMENT OF ACTIVE TUBERCULOSIS DISEASE: DOTS & MORE

Treatment of tuberculosis begins with a diagnosis. The main diagnostic test used in clinical care is a sputum smear microscopy test, which is inexpensive and can be performed in a matter of minutes. In this test, sputum (matter expelled from the lungs) is stained using carbol fuschsin and methylene blue and examined under a microscope *(7)*. The current treatment regimen focuses only on smear-positive tuberculosis cases.

Tuberculosis is treated with many drugs at a time, a practice known as combination therapy. Combination therapy has proven successful several decades and has proven successful; the use of many drugs prevents the TB bacteria from developing resistance to the entire drug regimen. Resistance to a single drug may develop, but because of its variety, the drug regimen will remain effective *(8)*.

The second support for combination therapy is that each of the TB drugs can have a different mode of action. Certain tuberculosis drugs have different properties under different conditions. The three main properties of anti-tuberculosis drugs are bactericidal activity (the ability of the drug to kill the bacteria), sterilizing activity (preventing the bacteria from reproducing) and finally the ability of the drug to prevent resistance to itself or other drugs. The six essential first line drugs are isoniazid, rifampicin, pyrazinamide, streptomycin, ethambutol and thioacetazone *(9)*. First line drugs are the first set used to treat a patient after their initial diagnosis; a patient receives a regimen of four of these six. If a resistance develops, the regimen can be altered. Tuberculosis treatment with antibiotics must be carefully controlled; when antibiotics are misused, multi-drug resistant tuberculosis can develop *(10)*.

If the infection develops a resistance to these drugs, the infection is called multi-drug resistance tuberculosis (MDR-TB), and second line drugs are used to treat it. However, these drugs are more expensive and have more severe side effects. Severe mistreatment of tuberculosis can lead to the development of extensively drug resistant tuberculosis (XDR-TB). This strain is even more difficult to treat than MDR-TB, and must be treated with third line drugs, which are more expensive and have more side effects than both the first and second line drugs *(11)*.

The first goal of tuberculosis treatment is to cure the patient of the disease and to prevent death from the disease or its late effects. The second goal is to prevent the relapse of tuberculosis following the treatment. The containment of the infection is also paramount, such that the patient does not spread tuberculosis to others. Finally, treatment aims to prevent the development of drug resistant strains of tuberculosis (MDR-TB and XDR-TB).

With this treatment ideology in mind, the World Health Organization launched the DOTS (Directly Observed Treatment, Short course) strategy for tuberculosis treatment in 1995. Originally the protocol was a regimen for six months for tuberculosis treatment. It has evolved to include advice on recommendations

to governments to tuberculosis treatment, including practices of managing treatment centres, diagnostic techniques such as sputum smear microscopy, and direct observation of patients' doses to ensure adherence to the treatment regimen. DOTS has become the foundation of tuberculosis treatment worldwide and has had much success in tuberculosis management. In 2010, the WHO reported that DOTS had successfully treated 86% of all new tuberculosis cases worldwide *(12)*, with successful treatment defined as either cured (a negative sputum bacteriology test) or treatment completed *(13)*.

Improving case detection rates (CDRs) is very important to the treatment and overall elimination of tuberculosis. The current goal of DOTS is to achieve and maintain a 70% CDR and to successfully treat 85% of the detected cases. In 2009, researchers at John Hopkins University constructed a computer model to test whether these short term reductions in TB incidence could be maintained in the long term, while maintaining these case detection and treatment rates. Indeed, the computer model showed that as case detection rates improved, the incidence of tuberculosis fell. However, as case detection rates stabilized, tuberculosis incidence, while still decreasing, would decrease by diminishing margins each year. From this model, researchers concluded that continuously trying to increase CDRs (above and beyond the 70% mark) is equally as important as quickly reaching a certain CDR goal *(14)*.

In improving CDRs, increased test frequency is already implemented as part of DOTS protocol *(15)*. Diagnostic test sensitivity can also be improved. The currently used sputum smear microscopy method only detects around 20-60% of cases even when properly implemented *(16)*.

In recent years, the non-profit organization, Foundation for Innovative New Diagnostics (FIND) has addressed the need for new tuberculosis diagnostics by issuing a plan outlining new tests they hope to develop and proposed deadlines for other development. FIND recognizes the need for tests at both the primary health care level and in the larger lab environment. For the clinical health post, it plans to develop a urine detection test – TB bacteria have been shown to be excreted in patients' urine and an antigen test may prove successful. For the laboratory setting, a set of liquid culture tests, dubbed the Mycobacterium Growth Indicator has been developed which will allow larger labs to identify the bacteria and test for the infection's drug susceptibility *(17)*.

NEW VACCINES

The Centre for Clinical Vaccinology and Tropical Medicine at the University of Oxford has developed a recombinant modified vaccinia virus, which has shown promise in phase 1 clinical trials. This vaccine is intended as a booster, meaning that when used in conjunction with BCG, it is intended to elicit a greater immune response. The vaccine is modified vaccinia Ankara, expressing antigen 85A (MVA85A). The phase 1 study showed that the MVA85A vaccine induced high levels of antigen-specific T cells when given to patients who had not received a BCG vaccination, thus producing the desired TB immunity through the TH1-type cellular immune response. When used within 24 weeks of a BCG vaccination, the increase in these antigen secreting T-cells was 5-30 times greater than BCG used alone. Measured is the amount of interferon gamma secreted by the T-cells, as shown by a tuberculin skin test and an antigen 85 response test (Fig. 1). As the graph shows, the count for patients vaccinated with both vaccines is higher than the count for those vaccinated with the two vaccines individually. Used in conjunction with BCG, this vaccine has the potential to offer anti-mycobacterial immunity in tuberculosis-endemic areas *(18)*.

Researchers at the University of Cape Town have tested the immunogenicity and safety of this new vaccine in South African patients. Monitoring patients for a year, they found that adverse reactions were limited to temporary swelling and redness around the injection site. Similar to the results of the previously mentioned , the results showed that the vaccine induced potent polyfunctional T-cell boosts. This study provided evidence that this vaccine has the potential to overcome the shortcomings of BCG (diminished efficacy due to patient's background mycobacterial exposure) *(19)*.

In 2009, Oxford researchers conducted the first study of any new vaccine in latent tuberculosis infected individuals. The results of the trial showed that there was no increase in adverse reactions in comparison to previous trials of non-tuberculosis infected individuals. The immune response generated was similar to the two previous trials *(20)*. The results of this study are important because since it is often not possible to detect LTBI in a clinical situation, the vaccine must be safe for these individuals as well *(18)*.

In addition to booster vaccines, recombinant strains of the original BCG vaccine are currently in development. The only recombinant vaccine currently investigated in human clinical trials is rBCG30, which secretes large amounts of the M. Tuberculosis 30 kDa major secretory protein. The introduction of this recombinant BCG vaccine causes the body to produce large amount of T-cells that respond to the 30 kDa protein. The proteins that the *Mycobacteria tuberculosis* secretes are composed of approximately 25% 30 kDa. It was therefore hypothesized that by causing the body to increase T-cell production specific to those proteins, the recombinant DNA strain increases protection against the TB bacteria *(19)*.

After initial trials in guinea pigs at UCLA, the vaccine was tested in phase 1 clinical trials by the Department of Internal Medicine at St Louis University. The double blind study randomly gave either the original BCG vaccine or the new recombinant vac-

cine to 35 healthy human subjects. rBCG30 induced a greater T cell response and an increased IFN-gamma secretion. Based on these results, researchers claimed that the recombinant strain can enhance human tuberculosis immunity. The data supports further development of this recombinant vaccine *(19)*.

HIV AND TB

HIV and tuberculosis coinfection is particularly deadly, and is not uncommon in certain parts of the world, especially Africa. The integration of tuberculosis and HIV treatment has started to yield positive results in some countries. The country of Malawi is currently a hotspot for HIV and tuberculosis coinfection, with a large percentage of the population infected with HIV and in need of antiretroviral therapy (ART). The HIV Unit, under the Department of Clinical Services, and the National Tuberculosis Program (NTP) have begun to work together; they established national guidelines and national policy for cotrimoxazole preventative therapy, the scale up of ART to deal with the HIV epidemic, and the co-administration of tuberculosis treatment and ART *(20)*.

A challenge faced by ART is that patients tend to not adhere to the treatment regimen. Combined treatments for the two infections calls for ART to begin after the initial intensive phase of tuberculosis treatment, and patients who receive tuberculosis treatment are often deterred from seeking ART. As patients feel better during the intensive phase of tuberculosis treatment, they feel no reason to seek ART for their HIV and so they tend to ignore this treatment. Evidence of this fact is that only 18% of patients receiving ART in Malawi have ever been diagnosed with tuberculosis; this is small in comparison with the fact that over 80% of tuberculosis patients are co-infected with HIV *(20)*.

CONCLUSIONS

The fight against tuberculosis is multi-faceted and fraught with issues spanning scientific research, environmental and logistical challenges, and government policy. The existing DOTS protocol has been shown to be successful. The continued implementation of this strategy will result in decreased tuberculosis incidence and will greatly further the goal of eliminating this epidemic. In addition to the continued support of the DOTS strategy, there are a few other scientific developments that have been discussed that can contribute to fighting the tuberculosis epidemic. The booster vaccine MVA85A has shown promise in trials, but it is still decades away from implementation, during which other phases of clinical trials must take place.

The implementation of new diagnostic tests, such as those being developed by FIND, will allow case detection rates to increase by increasing diagnostic sensitivity and test frequency. Based on the computer models discussed earlier, the continuous increase of these rates is necessary if tuberculosis is to be eliminated. Additionally, the continued integration of HIV and tuberculosis treatment centers can improve patient care and increase adherence to treatment.

The current tuberculosis epidemic has a huge array of challenges that must be overcome before this epidemic can be stopped. The steps taken by the World Health Organization thus far have attempted to decrease the severity of the epidemic; however an end is still a long way off. The current plan by WHO has an optimistic goal of ending the epidemic by 2050; with both their commitment and that of the scientific community, hopefully this goal can be realized.

REFERENCES

1. "Tuberculosis Fact Sheet" (World Health Organization, Geneva, Switzerland, 2008).
2. "The Stop TB Strategy" (World Health Organization, Geneva, Switzerland 2006).
3. G. Friedland, G. Churchyard, E. Nardell. *J. Infect. Dis*. **196**. S1-S4 (2007).
4. V. Kumar, A.K. Abbas, N. Fausto, R. Mitchell. *Robbins Basic Pathology (8th Ed)* (Saunders, Philadelphia, 2007).
5. "Global Tuberculosis Control: Epidemiology, Strategy, Financing" (World Health Organization, Geneva, Switzerland, 2009).
6. G. Black, *et al. Lancet* **359**, 1393-402 (2002).
7. "TB Dots: Doctor's Section - TB- Diagnosis" (Sandoz, Holzkirchen, Germany, 2006).
8. "Treatment of Tuberculosis: Guidelines for National Programmes" (World Health Organization, Geneva, Switzerland, 2003).
9. "Global Tuberculosis Control: Epidemiology, Strategy, Financing" (World Health Organization, Geneva, Switzerland, 2009).
10. "Treatment of Tuberculosis: Guidelines for National Programmes" (World Health Organization, Genva, Switzerland, 2003).
11. "WHO | Global Tuberculosis Control 2010" (World Health Organization, Geneva, Switzerland, 2003).
12. H. Cox, M. Morrow, and P. Deutschmann. *BMJ* **336**, 336-484 (2008).
13. D. Dowdy, R. E. Chaisson. *Bull. WHO* **87** 296-304 (2009).
14. M. D. Perkins, G. Roscigno, and A. Zumla. *Lancet* **367**, 942-43 (2006).
15. "FIND: Tuberculosis" (Foundation for Innovative New Diagnostics, Geneva, Switzerland, 2010)
16. H. McShane, *et al. Nature Med*. **10**, 1240 (2004).
17. T. Hawkridge, *et al. J. Infect. Dis*. **198**, 544-52 (2008).
18. C. R. Sander, *Am J Respir Crit Care* **179**, 724-33 (2009).
19. M. A. Horwitz. "Recombinant BCG Expressing Mycobacterium Tuberculosis Major Extracellular Proteins" (Univ. of Cal: Los Angeles, Los Angeles, 2005)
20. G. Friedland, A. Harries, D. Coetzee. *J. Infect. Dis.* **196**, S114-123, (2007).

The effect of familiarity on vigilance behaviour in grey squirrels

Julia Shonfield*[1]

[1]Department of Biology, McGill University, 1205 Avenue Docteur Penfield, Montreal, Quebec, Canada H3A 1B1

ABSTRACT

Introduction: Vigilance enables an animal to obtain information about the environment but often at a cost of reduced foraging rate. Some environmental information may not change rapidly, so vigilance might be safely reduced with familiarity with an area. Studies have noted this decline in vigilance with familiarity, but the reason for this decline has not been tested. **Methods**: I proposed and tested two hypotheses to explain this decline in vigilance. The Safe Experience hypothesis suggests the probability of a predator being nearby but undetected decreases with time spent in an area, enabling an animal to decrease its vigilance due to the reduced risk. The Visual Experience hypothesis suggests that as time progresses vigilant animals acquire more information from their surroundings (e.g. refuge locations) allowing for a decrease in vigilance because an animal would not need to detect a predator as early if reaching a refuge required less time. Grey squirrels (*Sciurus carolinensis*) were used to test these hypotheses by feeding them peanut butter in an apparatus that limited their access to visual information by varying degrees. **Results**: An effect of familiarity was evident by a sharp decline in vigilance rates within trials. Squirrels adjusted vigilance postures to the different treatments, but the rate of decline in vigilance was unaffected by treatment. **Discussion**: While vigilance is related to visual information, the decline in vigilance with familiarity is not related to the amount of visual information obtained from the environment, giving provisional support to the Safe Experience hypothesis.

KEYWORDS

Vigilance, foraging, familiarity

*Corresponding author:
julia.shonfield@gmail.com

Received: 2 January 2011
Revised: 8 March 2011

INTRODUCTION

The act of vigilance enables an animal to obtain information on its surroundings *(1)*, such as information on nearby refuges, escape routes, predator approaches, and conspecifics *(2)*. Unfamiliar environments have been found to elicit higher vigilance *(3, 4)*, likely because potential sources and locations of danger, as well as locations of refuge, are not known. Familiarity with an area is important for survival because an animal can benefit from knowing the types and locations of food *(5)* and refuge *(6)* available. Animals in unfamiliar locations take longer to find refuge *(7-9)*, and consequently are at higher risk of predation *(6, 7, 10, 11)*.

Previous studies have found that vigilance decreases with increased familiarity with the surroundings: in Holstein dairy cows *(4)*, eastern chipmunks, *Tamias striatus (3)*, grey squirrels, *Sciu-*

rus carolinensis (12) and barbary doves, *Streptopelia risoria (13)*. However, there has been little consideration of why this decrease in vigilance occurs, and consequently no studies have attempted to predict what affects the relationship between vigilance and familiarity. The decrease in vigilance could be related to the increase in knowledge of the surroundings (such as refuge locations) with time, or the decrease in vigilance could be related to predation risk as the probability that a predator is present but undetected decreases with time spent in an area *(3)*.

In this study, I proposed and tested two hypotheses to explain this decrease in vigilance. The Safe Experience hypothesis suggests that since the probability of a predator being nearby but undetected decreases with time spent in an area, an animal can decrease its time spent being vigilant, because of the lower risk of no predators in the vicinity, and the arrival of a predator would involve movement that would be more easily detected *(11, 14)*. The Visual Experience hypothesis suggests that the more time an animal spends being vigilant, the more information is obtained from the surroundings (e.g. location of refuges and escape routes). This leads to a decrease in vigilance, as the knowledge of possible refuges allows for a slightly later detection of a predator. The Visual Experience hypothesis predicts that vigilance will decrease as the amount of visual information obtained from the surroundings increases, whereas the Safe Experience hypothesis predicts a decrease in vigilance regardless of the amount of visual information obtained.

To distinguish between these hypotheses, I studied the effect of familiarity on vigilance in grey squirrels (*Sciurus carolinensis*) during visits to a food patch, using a feeding apparatus with walls of varying heights (treatments). The apparatus added two elements of unfamiliarity to the environment: it was a novel object and a novel food patch for the squirrels. The different treatments made it possible to vary the amount of visual information that could be obtained by being vigilant. The Visual Experience hypothesis predicts differences between treatments on the rate of decline in vigilance, because if familiarization is affected by visual information then more rapid familiarization would be expected when the amount of visual information obtained is greater. Conversely, the Safe Experience hypothesis predicts no difference between treatments on the rate of decline of vigilance since the rate is independent of the amount of visual information obtained from the surroundings.

I also looked at whether the type of vigilance posture was affected by access to visual information. Squirrels exhibit several different vigilance postures of varying heights (in a range from quadrupedal to bipedal postures *(15)*, that allow them to get a better view of their surroundings by increasing their viewing range *(16)*. I expected squirrels to adjust their vigilance postures to the different wall heights of the different treatments, based on the assumption that access to visual information influences vigilance posture.

METHODS

EXPERIMENTAL APPARATUS

The experimental apparatus consisted of three walls positioned around a food source (Fig. 1), a glass plate with 30ml of evenly spread smooth peanut butter. As grey squirrels have been shown to be vigilant while handling food items in a bipedal position *(12)*, the peanut butter setup forced squirrels to eat with their

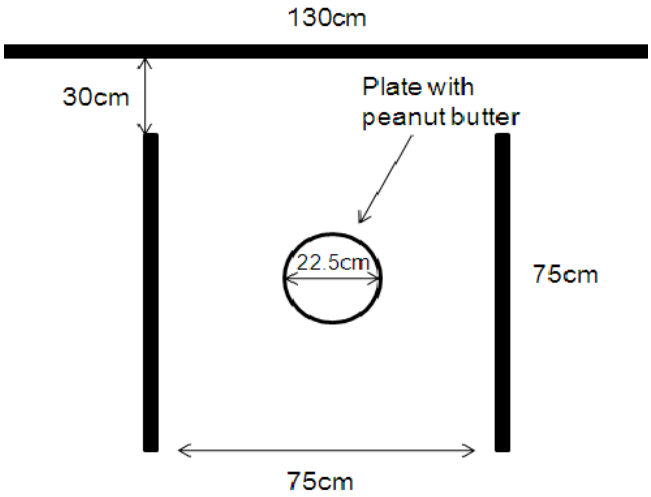

Fig 1. The design and spatial layout of the experimental apparatus (seen from above) used to test the effect of familiarity on vigilance. The height of the walls surrounding the food source varied with the different treatments: 6cm for the low walls treatment, 15cm for the medium walls treatment, and 40cm for the high walls treatment.

Posture	Type	Description
Low head raise	Quadrupedal	Head raised with eyes below the highest part of the squirrel's back
High head raise	Quadrupedal	Head raised with eyes above the highest part of the squirrel's back
Semi-upright	BIPEDAL	Sitting on back feet with back noticeably arched
Upright	Bipedal	Sitting on back feet with back straight, more fully upright than the semi-upright posture

Table 1. Descriptions of the different vigilance postures exhibited by grey squirrels.

heads down. Each wall of the apparatus consisted of two wooden poles pounded into the ground, with black gardening fabric stretched between them. Once the squirrel entered the apparatus, the walls blocked the squirrel's view in three directions. The open end of the apparatus provided a clear view to videotape the vigilance behaviour of the squirrel. The apparatus did not have a roof because previous studies using overhead blocks found they have no effect on vigilance *(12, 17, 18)*.

Four different treatments were used with varying wall heights: low walls were 6cm in height, medium walls were 15cm in height, and the high walls were 40cm in height. The fourth treatment consisted of only the plate with peanut butter (referred to as the 'no walls' treatment). The design of the low and medium walls treatment was such that squirrels could still obtain information from their surroundings if they adjusted their vigilance posture to the wall height. Based on a few pilot trials, I determined that squirrels were able to see over the low walls using a quadrupedal vigilance posture, and squirrels were able to see over the medium walls using a bipedal vigilance posture. The high walls treatment blocked the squirrel's view even in bipedal vigilance postures.

FIELD TRIALS

Study sites were located in several Montreal parks, with 3 trials in the area surrounding Lac aux Castors on Mont Royal, 14 trials in Angrignon Park, and 19 trials in Maisonneuve Park. Trials were conducted in open grassy areas where trees were spaced more than 3m apart. I conducted a total of 36 trials were conducted between 10:00 and 16:00 h from October 21 to December 2, 2006, on days without rain.

I conducted trials in sets of the four treatments to keep samples sizes consistent across treatments (9 trials in each treatment), with the order of the treatments and the orientation of the open end of the apparatus (north, east, south or west) randomized in each set. I attracted a squirrel to the apparatus by throwing a couple nuts (either peanuts or sunflower seeds) towards the apparatus. For each trial I set up the apparatus 2-5m from a large tree (> 20cm in diameter), and filmed the behaviour of the squirrel with a video camera (Panasonic Digital Palmcorder, PV-DV400-K) on a tripod positioned 10m from the open end of the apparatus. Trials were spaced at least 100m apart to minimize the likelihood of retesting the same individual. The trial began when the squirrel first entered the apparatus (no prior familiarization), and ended when the squirrel exited the apparatus of its own accord to forage or in some cases was chased out of the apparatus by a conspecific or domestic dog (*Canis familiaris*). I minimized interruptions of trials by conspecifics by distracting other squirrels in the vicinity with nuts (peanuts, sunflower seeds, and hazelnuts).

DATA EXTRACTION AND ANALYSIS

From each videotaped trial, I counted the number of vigilance bouts in each minute to get a rate of vigilance per minute, which was used as the response variable in subsequent analyses. Only the first three minutes were analyzed because of small sample sizes after three minutes (i.e. most squirrels exited the apparatus after three minutes). Each vigilance bout was classified into one of several different posture types (Table 1), as previously described in other studies on vigilance behaviour in squirrels *(15, 19)*. Nonparametric tests were used because the data were not normally distributed (Shapiro-Wilk normality test, $p<0.001$). Statistical analyses were done using SYSTAT® Version 12, with an alpha significance level of 0.05.

RESULTS

THE EFFECT OF TIME AND TREATMENT

Vigilance rates were similar between treatments, with all four treatments showing a sharp decline in vigilance rate from the first to the second minute, and remaining relatively constant from the second to the third minute (Fig. 2). There were no significant differences in vigilance rates in the first three minutes of trials between different treatments. (Kruskal-Wallis test: 1st minute interval $H_3=3.239$, $p=0.356$; 2nd minute interval $H_3=1.933$, $p=0.586$; 3rd minute interval $H_3=4.942$, $p=0.176$). Since treatment had no effect on vigilance, all treatments were combined to test for the effect of time. Time had a strong effect on vigilance rate (Friedman test: $Q=17.721$, $p< 0.001$), and vigilance rate sharply declined by 62% from the first to the second minute (Wilcoxon signed ranks test: $p<0.001$). The rate of vigilance remained relatively constant after the first minute and there was no significant difference in vigilance rate during the second and third minute (Wilcoxon signed ranks test: $p=0.5$).

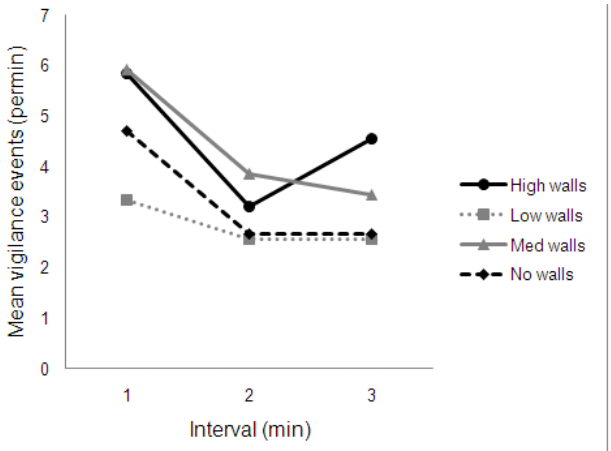

Fig 2. Mean number of vigilance events per minute for each of the four treatments for the first three minutes of each trial.

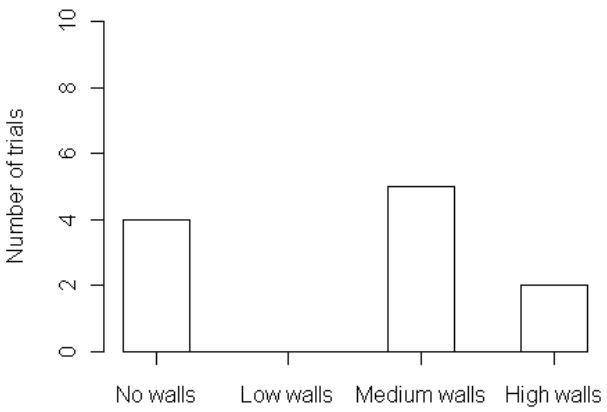

Fig 3. Number of trials with the occurrence of either of the two bipedal vigilance postures (semi-upright and upright).

VIGILANCE POSTURES

The quadrupedal vigilance postures, the low and high head raises (Table 1), were the most common types of vigilance postures. The different treatments ranged from a mean of 90%-100% quadrupedal postures out of the total number of vigilance postures that occurred in the first three minutes of each trial. Bipedal vigilance postures, semi-upright and upright, were used less often and accounted for a mean of 0-10% bipedal postures out of the total vigilance postures that occurred in the first three minutes of each trial. The number of trials where the squirrel used bipedal vigilance postures differed between the treatments (G test of independence: G=10.051, p=0.018; Fig. 3).

DISCUSSION

Squirrels responded to the various treatments by modifying their vigilance postures to the different wall heights. The occurrence of bipedal vigilance postures (semi-upright and upright) differed between treatments, with bipedal postures occurring more frequently in trials with the medium walls treatment and less frequently in the low walls and high walls treatment. This was expected because the medium walls treatment was the only treatment that allowed better access to visual information with the use of bipedal vigilance postures. Quadrupedal vigilance postures were sufficient to see over the walls in the low wall height treatment, and in the high walls treatment neither vigilance posture was effective in accessing visual information. The no walls treatment also had a high occurrence of bipedal postures, and although it is not clear why this was the case, it might have been due to uncontrolled environmental factors such as grass height, or other vegetation that might have affected access to visual information in these trials. My results support previous evidence that vigilance postures are related to the gain of visual information. They are consistent with other studies that found bipedal postures were used more often in habitats where better views of the surroundings could be gained by their use of bipedal postures.

Vigilance rates declined sharply (62%) with increased time feeding in the apparatus, primarily between the first and second minute of the trials. This suggests that familiarization in grey squirrels in an urban setting occurs mainly in the first minute of exposure to a novel situation. Other studies have found an effect of familiarity between repeated visits to a novel location where food was provided. For example, a study on dairy cows found a 41% decrease in the time spent vigilant over 11 trials *(4)*, and a study on barbary doves found an 80% decrease in time spent vigilant over 7 trials *(13)*. A study on eastern chipmunks also found a significant decline in vigilance among successive trips to a food patch *(3)*. There is almost no previous evidence, however, for familiarity affecting vigilance over the course of a single visit to a food patch (which has been demonstrated in this study). In a study on eastern chipmunks, a non-significant decline in vigilance rate within a single visit to the food patch was documented; however, the chipmunks made three familiarization trips to the food patch prior to data collection *(3)*.

CONCLUSION

I found that varying access to visual information had no effect on vigilance rates of grey squirrels over the first three minutes of the trials, giving provisional support to the Safe Experience hypothesis. This suggests that the decline in vigilance in grey squirrels due to familiarity is not a result of increased information about the surroundings, but is instead due to a presumed decrease in predation risk as an animal forages without any sign of a predator in the vicinity. Although more work in this area is necessary to conclude with certainty which hypothesis best explains the decline in vigilance with familiarity, this study provides the first step in establishing how familiarity affects vigilance by proposing and testing hypotheses to explain the observed decrease in vigilance rate. The approach used in this study of varying the amount of visual information and the design of the apparatus provides a useful way of testing for effects of familiarity and could be important for later studies addressing similar questions.

This study was done on grey squirrels in an urban setting, and the results on the effects of familiarity raise an interesting question as to whether there are differences between grey squirrels in urban and natural areas in regards to the time it takes to become familiar with their surroundings. It is possible that the effect of familiarization on vigilance behaviour would differ between squirrels in urban areas and squirrels living in natural areas because of different stimuli from their environments and differences in preda-

tory risk *(21)*. Familiarization might play an important role for animals adapting to urban environments, since novel situations may occur more often and animals that familiarize more quickly could benefit by decreasing their foraging costs.

ACKNOWLEDGEMENTS

I would like to thank Donald Kramer for his guidance throughout all stages of this research. I would also like to thank Joanna Makowska for technical advice for the field work part of this project, Henri Valles for statistical advice, and Geoff Sherman for help with the construction of the apparatus and for helpful comments on this manuscript.

REFERENCES

1. S. Dimond, J. Lazarus, *Brain, Behaviour and Evolution* **9**, 60 (1974).
2. P. Y. Quenette, *Acta Oecologica-International Journal of Ecology* **11**, 801 (1990).
3. W. Trouilloud, A. Delisle, D. L. Kramer, *Animal Behaviour* **67**, 789 (Apr, 2004).
4. T. Welp, J. Rushen, D. L. Kramer, M. Festa-Bianchet, A. M. de Passille, *Applied Animal Behaviour Science* **87**, 1 (Jul, 2004).
5. J. Pusenius, R. S. Ostfeld, F. Keesing, *Ecology* **81**, 2951 (Nov, 2000).
6. K. W. Larsen, S. Boutin, *Ecology* **75**, 214 (Jan, 1994).
7. L. H. Metzgar, *Journal of Mammalogy* **48**, 387 (1967).
8. M. F. Clarke *et al., Oikos* **66**, 533 (Apr, 1993).
9. J. J. Jacquot, N. G. Solomon, *American Midland Naturalist* **138**, 414 (Oct, 1997).
10. J. M. Yoder, E. A. Marschall, D. A. Swanson, *Behavioral Ecology* **15**, 469 (2004).
11. P. R. Sievert, L. B. Keith, *Journal of Wildlife Management* **49**, 854 (1985).
12. I. J. Makowska, D. L. Kramer, *Animal Behaviour* **74**, 153 (Jul, 2007).
13. J. P. Desportes, A. Gallo, F. Cezilly, *Behavioural Processes* **24**, 177 (Nov, 1991).
14. G. Martel, L. M. Dill, *Ethology* **99**, 139 (Feb, 1995).
15. C. L. Arenz, D. W. Leger, *Animal Behaviour* **57**, 97 (Jan, 1999).
16. M. J. Hannon, S. H. Jenkins, R. L. Crabtree, A. K. Swanson, *Journal of Mammalogy* **87**, 287 (Apr, 2006).
17. C. L. Arenz, D. W. Leger, *Behaviour* **134**, 1101 (Nov, 1997).
18. I. J. Makowska, D. L. Kramer, *Animal Behaviour* **74**, 153 (Jul, 2007).
19. C. L. Arenz, D. W. Leger, *Ethology* **105**, 807 (Sep, 1999).
20. P. B. Sharpe, B. Van Horne, *Journal of Mammalogy* **79**, 906 (Aug, 1998).
21. M. A. Bowers, B. Breland, *Ecological Applications* **6**, 1135 (Nov, 1996).

Atmospheric circulation structures associated with freezing rain in Quebec City, Quebec

Sophie Splawinski*[1], John R. Gyakum[1], Eyad H. Atallah[1]

[1]Department of Atmospheric and Oceanic Sciences, McGill University, 805 Rue Sherbrooke West, Montreal, Quebec, Canada H3A 2K6

ABSTRACT

Introduction: An analysis of freezing rain (FZRA) events in Quebec City (YQB), Quebec, Canada, a climatologically active area, is counted over a 30 year period (1979-2008) in an attempt to better understand the synoptic patterns, severity, and frequency of such events. **Methods**: Of the 218 individual events, 48 are classified as severe and are given a more in depth analysis at various pressure levels. Events are partitioned into five categories based on synoptic patterns, including the location and organization of surface features, 500 hPa trough location and length, and instantaneous geostrophic wind direction at YQB at the first hour of reported FZRA. Composite analyses of atmospheric variables are then created for each category, and the latter are then compared. **Results**: Each of the five categories has a unique thermodynamic and dynamic signature. Identifying these signatures within forecast models may significantly improve the prediction of freezing rain events. **Discussion**: FZRA events have not been studied extensively in the SLRV and so identifying these aforementioned signatures within forecast models may significantly improve the prediction of freezing rain events.

KEYWORDS

Meteorology, freezing rain (FZRA), severe weather, synoptic scale, Quebec City.

*Corresponding author:
sophie.splawinski@mail.mcgill.ca

Received: 1 January 2011
Revised: 12 March 2011

INTRODUCTION

MOTIVATION

The St-Lawrence River Valley (SLRV) is one of the more climatologically active areas for freezing rain (FZRA) in North America. Associated inconveniences with freezing rain range from small scale disruption of ground transportation and aircraft operations to a large scale regional shut down *(8)*. Quebec City (YQB) is located in the St-Lawrence River Valley (SLRV), a primary topographic feature of eastern Canada, extending in a southwest-northeast direction from Lake Ontario, past Montreal (YUL) and Quebec City (YQB) to the Gulf of St-Lawrence *(7)*. The 1998 ice storm was the most devastating natural disaster in Quebec history. Data provided by the National Oceanic and Atmospheric Administration indicates that the storm killed 44 people and caused nearly $4 billion of damage in the United States and Canada *(6)*.

OBJECTIVES AND MOTIVATION

This paper attempts to identify synoptic-scale, a horizontal length scale on the order of 1000km, circulation structures associated with ice storms in Quebec City. Current forecasting techniques include analyses of the expected vertical profile of the atmosphere using skew-t diagrams or tephigrams, in conjunction with surface and upper level movement of low-pressure systems as they approach the province of Quebec. However, the dynamics and thermodynamics of these events within the SLRV have not been studied extensively. Although Quebec City escaped most of the devastating effects of the 1998 ice storm, it shares a similar history of FZRA occurrences with its southwestern counterpart, Montreal (YUL). Quebec City is a large metropolitan area, housing almost 500,000 people. It is imperative to increase understanding of the physical processes occurring in these freezing rain events, to increase the safety of the public.

PREVIOUS WORK

Freezing precipitation can form through two microphysical paths *(9)*: the melting process and the collision-coalescence process. The first path forms FRZA, and the second creates freezing drizzle. This paper will focus solely on FZRA as previous research shows *(5,3,11)* that the synoptic-scale patterns associated with freezing drizzle may differ from those associated with freezing rain *(6)*.

Few studies conducted in eastern Canada examine the type and frequency of synoptic-scale weather patterns associated with freezing precipitation *(9)*. Most studies that are conducted revolve around either a climatology or case studies of one severe event. Since YQB is located in the SLRV, it is subject to pressure-driven channeling of surface winds throughout all seasons. YUL and YQB exhibit countercurrents where the direction of the wind within the valley is opposite to the wind above the valley *(7)*. Pressure-driven channeling refers to valley winds that are driven by the pressure gradient along the valley axis.

RESULTS

APPROACH

In order to adequately investigate freezing rain occurrences, it is necessary to define a severe event. The 30-year period (1979-2008), analyzed using hourly surface observations from Environment Canada's Digital Archive of Canadian Climatological Data, had a total of 218 individual events. Individual events are defined as continuous or intermittent freezing rain precipitation lasting at least one hour. If non-freezing rain reports between FZRA events exceed six hours, the next FZRA report is considered a new event. A severe event is categorized as having six or more hours of freezing rain using the same guidelines as set for individual events. Of the 218 total events recorded, 48 were found to be severe. Events are classified using partitioning methods, discussed below, and composites are created for each category. Composites consist of an average field of analyses taken for individual events over the first hour of reported FZRA. The partitioned synoptic-scale composite identifies potential triggers and signatures, which may be used by forecasters to identify future freezing rain events at YQB.

DATA

Freezing rain events at the Jean Lesage International Airport in Quebec City (YQB) were identified using hourly surface observations from Environment Canada's Digital Archive of Canadian Climatological Data. Events occurred from the months of November and April, inclusively, throughout the 30 specified years (1979-2008).

The North American Regional Reanalysis (NARR) dataset *(2)* was then used in conjunction with the General Meteorological Package (GEMPAK) version 5.7.11 to produce most of the analyses and graphics. The NARR uses the NCEP North American Mesoscale model, which has a 32-km horizontal grid with 45 vertical layers and analyses performed every three hours *(4)*.

The Air Resources Laboratory Hysplit Trajectory Model was employed with a matrix grid of two-degree latitude-longitude separation to illustrate the paths of 24 trajectories at three different levels. Levels were chosen at 300m, 3000m, and 5500m corresponding to the approximate respective pressure levels of 1000hPa, 700hPa, and 500hPa. These levels were found to best represent incoming air parcels in the distinct low-level cold layer and mid-level warm layers of a FZRA event. Backward trajectories traced back in time to 84 hrs prior to the first report of freezing rain were chosen to better understand the origins of the air parcels.

METHODS AND PARTITIONING TECHNIQUE

We constructed Fig. 1 using the Air Resources Laboratory Hysplit Trajectory Model. The upper panel of each category displays horizontal parcel displacement and the lower panel displays vertical displacement as a function of time. The 3000m level, coinciding with the warm layer, provides a basis for partitioning. Categorization is based on the range of altitudes at which air parcels begin.

A large-scale analysis of various atmospheric variables at different levels which track the progression of the system responsible for the freezing rain in Quebec City yields a better understanding of its development and life cycle. Furthermore, the partitioning technique employed when categorizing severe events allows for a more dynamic, comprehensive, time-integrated approach

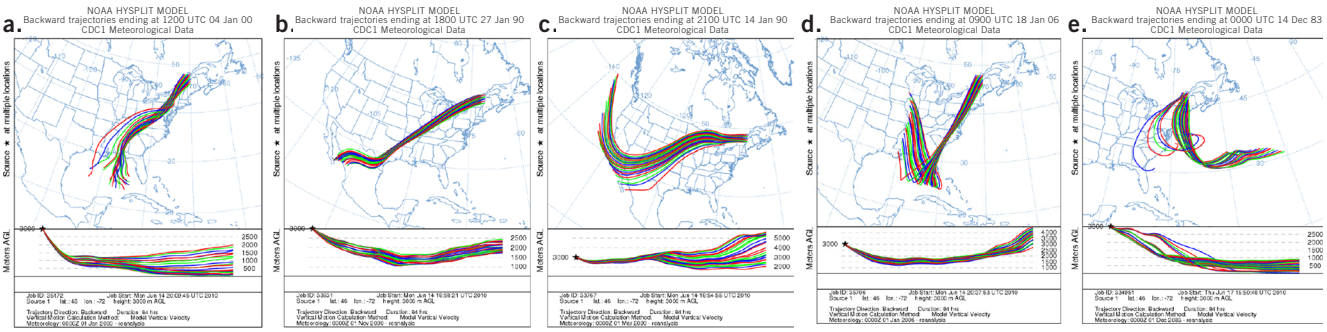

Fig 1. From left to right: LL, ML, UL, EC, CP parcel trajectories, one event taken from each category. The lower panel provides the approach for partitioning based on the range of altitudes at which air parcels begin.

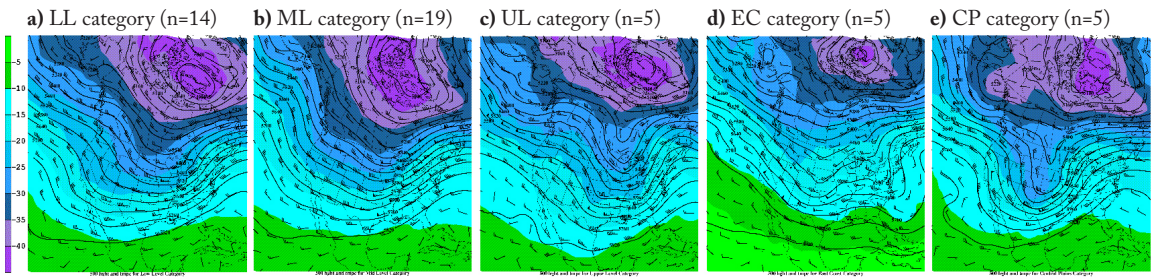

Fig 2. Composite analyses of 500hPa height (black contours, interval: 40m) and temperature(°C, shaded).

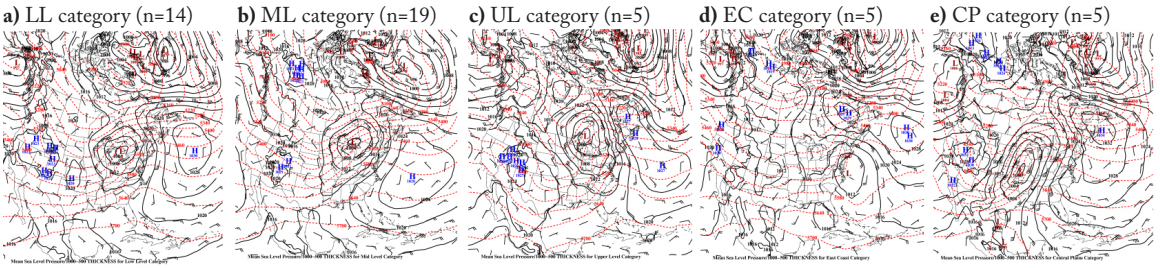

Fig 3. Mean sea level pressure (hPa, black contours are isobars with interval 4 hPa) composites illustrate the spatial pattern of couplets associated with each category. Wind barbs indicate surface wind speeds, red dashed lines indicate 1000-500 hPa thickness (contour interval of 60m).

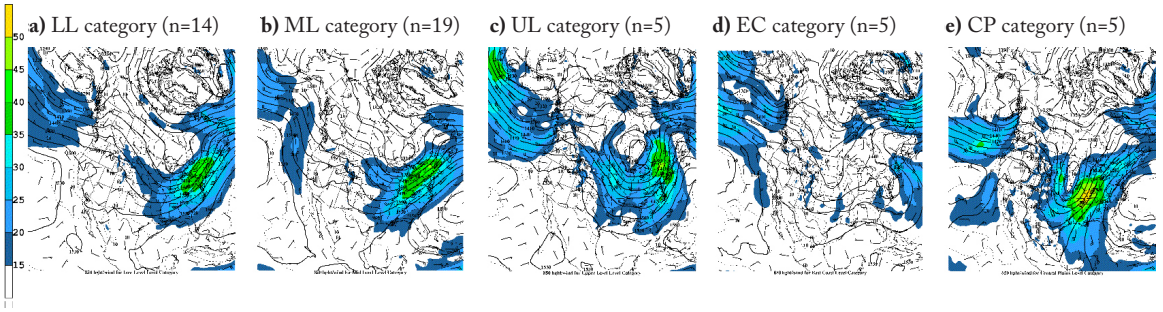

Fig 4. 850 hPa Temperature (°C, shaded) and 850 hPa height (contour interval of 30m) composites for each category.

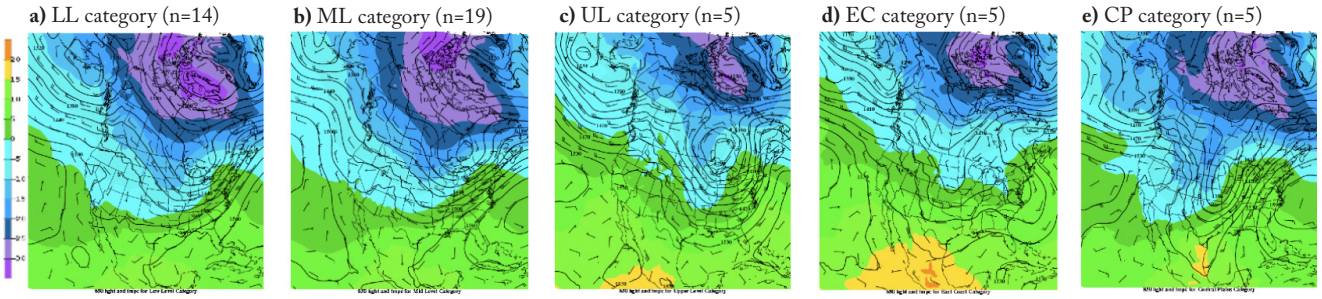

Fig 5. 850 hPa Temperature (°C, shaded) and 850 hPa height (contour interval of 30m) composites for each category.

compared to specifically looking at one time frame of the system's development. By looking at parcel trajectories, we get an 84h progression on both the horizontal and vertical planes. The progression is then correlated to two synoptic spatial patterns observed at the initial onset of FZRA at YQB, explicitly at the surface and at 500 hPa. Surface observations also indicate that a specific instantaneous geostrophic wind direction is present within each category. Geostrophic winds blow parallel to isobars, contours of constant pressure, and refer to winds balanced by the pressure gradient and coriolis forces. Categorization is therefore based on both a static and dynamic approach, here providing a sound and diverse method of partitioning, the most important step in the research of FZRA at YQB. Five examples, one from each category, are given in Fig. 1 (a,b,c,d,e shown as Low Level (LL), Mid Level (ML), Upper Level (UL), East Coast (EC), and Central Plains (CP), respectively).

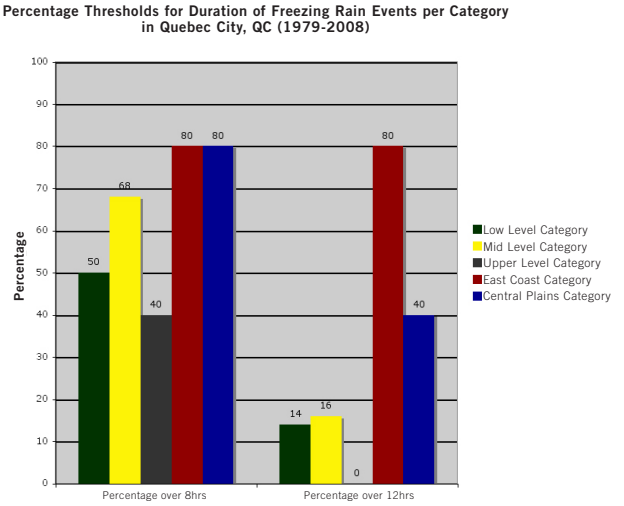

Fig 6. Threshold Duration of FZRA per category.

COMPOSITES

Composites consist of an average of individual analyses of events present in each category. Each individual analysis is constructed at the onset of FZRA precipitation at YQB. The 500 hPa height temperature field (Fig. 2) shows all five categories with an environment conducive to synoptic-scale ascent over YQB— situated downstream of a height trough. The UL category is centered over Ontario whereas the CP category is centered over Manitoba. The EC category is most notably distinguished by a negatively tilted short-wave trough along the East Coast of the United States.

The sea-level pressure and 1000-500 hPa thickness fields (Fig. 3) exhibit cyclone-anticyclone couplets providing distinct instantaneous geostrophic winds at YQB. These winds coincide with air parcel trajectories at both 300m and 3000m for their respective events. The EC category is uniquely characterized by easterly geostrophic flow at YQB, with a north-south anticyclone-cyclone couplet. The other composites are primarily characterized by southerly geostrophic flow at YQB, with a west-east cyclone-anticyclone couplet.

A 850hPa wind speed (kts) isotach analysis (Fig. 4) pinpoints the presence of a low level jet, defined by speeds exceeding 15kts, in each category. The strongest winds, 30 kts above the climatological average, are associated with the CP category. All categories, except for that of the EC, have winds that are 1 to 2 standard deviations above the normal range (15-25kts), indicating large amounts of warm air and moisture transport from the south. The EC category retains its high moisture transport due to the trajectories' proximity to the Atlantic Ocean.

Geostrophic warm advection at 850-hPa over YQB (Fig. 5) provides favorable conditions for ascent. The persistence of warm air advection, the temperature increase associated with the transport of warmer air into the region of interest, and moisture transport over YQB supports FZRA formation and maintenance. The UL and EC categories have the warmest associated mean (ranging to 5°C). Owing to the UL category's meridional flow, FZRA duration is shortest with respect to all other categories, regardless of the presence of much higher maximum 850 hPa temperatures.

Figure 6 presents percentage threshold duration of FZRA events per category. Thresholds are set at 8 and 12h respectively. The EC category has the longest duration of events, with 80% of events lasting over 12h. On the other hand, the UL category has no events lasting over 12hrs, as well as only 40% of all events lasting over 8 hrs.

DISCUSSION

A major focus of our research is to determine synoptic patterns that influence the duration of FZRA. Ideal conditions require a deep warm layer, with temperatures above 0°C, maintained with warm air advection. This yields a constant influx of moisture and above zero temperatures. The progression of spatial patterns at the surface, 850 hPa, and 500 hPa, bracket the potential interval of duration of each event. As outlined by Cheng *et al. (1)*, duration thresholds, chosen to be 8 and 12h, are used to determine variability among the categories. The longest events are found in the EC and CP categories. Moreover, 80% of all EC events last over 12h, coinciding with conclusions reached by Rauber *et al. (9)*: "processes occurring on the cold side of moving and stationary warm fronts and deep within EC air masses were most efficient at producing freezing precipitation per unit area."

The EC category produces ideal conditions to allow the maintenance of this structure. A time-scale analysis of events tracking up the coastal United States provides markers that depict constant and persistent moisture and temperature transport at 850 hPa, and constant low-level influx of cold air. The influx of cold air is significant as microphysical processes related to the release of latent heat associated with freezing rain often disrupt this layering process. The essentially meridional track of low pressure systems within this category, as opposed to the more typical zonal track, allows for eastward-located warm sector to be maintained at mid levels for a longer period of time. Furthermore, the anticyclone located over Northern Quebec channels near-surface arctic air, representing the lowest portion of the Earth's atmosphere, with a depth ranging from 8 to 17km in the mid-latitudes, into the SLRV providing the cold air necessary for the maintenance of FZRA. The North-South couplet of mean sea level pressure provides a basis for a blocking pattern, while the negatively-tilted shortwave trough allows for the intense deepening of the low pressure system. Though low level jet winds are closely approximated by the climatological mean, moisture trajectories stemming from the Atlantic travel a short distance to YQB, allowing for an availability of substantial precipitable water.

Additionally, the CP category also yields events of especially long duration. Specifically, this category is characterized by 40% of its events lasting over 12h. Synoptic patterns indicate that moisture and warm air advection originate in the Gulf of Mexico. Although this is a significant distance to cover, it is quite feasible given that this category is characterized by the highest 850 hPa wind speeds among all categories, with top speeds exceeding 50 kts. For comparison purposes, a 60 kt wind transports moisture in the atmosphere for a distance of approximately 110 km in an hour. The trajectory of the low pressure system allows for the maintenance of the mid level warm layer, as the warm air mass ahead of the low air mass covers much of the Eastern United States. This results in a warm sector whose area has more coverage in Canada than the LL, ML, and UL categories. The Southwest-Northeast couplet at sea level also provides ideal wind channeling conditions to maintain the surface cold layer's maintenance.

Unlike the LL and ML categories, which hold similar duration intervals, the UL category yields no events lasting over 12h. Analysis of 500 hPa, 850 hPa, and surface composites provides a synoptic reasoning for this result. The meridional shortwave trough present at 500hPa in UL cases is not conducive for a long-term maintenance of the mid level influx of warm air, as the track of the associated surface low quickly brings about the encroaching arctic air on the backside of the cold front. Loss of mid level influx of warm air results in a phase change in precipitation from FZRA to snow. Furthermore, although 850 hPa temperatures and wind speeds are warmer and stronger than those of the other categories, their small coverage of area yields a shorter duration of FZRA.

CONCLUSION

Severe FZRA events in the Quebec City area are associated with specific synoptic patterns, partitioned into five categories. The intensity and duration of these events are connected to the spatial distribution of the associated atmospheric patterns. East Coast cases are associated with particularly long durations, with 80% of these events lasting longer than 12h. Events in the Central Plains category represent a large portion of longer lasting events, with 40% lasting over 12h.

A major limitation of this study is the lack of FZRA accumulation values. Environment Canada does not directly record accumulation amounts for freezing rain. Instead, they use a chart which consists of light ($< 2.5\ mmh^{-1}$), moderate ($2.5\text{-}7.5 mmh^{-1}$), and heavy ($> 7.5 mmh^{-1}$) precipitation. It was therefore necessary to employ a less precise method of categorization based on total duration instead of precipitation rates.

This analysis of synoptic signatures associated with FZRA events in Quebec City provides meteorologists and researchers with a new documentation of synoptic-scale patterns over the area.

These results are an important step in better understanding the formation, progression, and duration of a severe natural phenomenon that can wreak havoc on major cities, infrastructure, and citizens.

ACKNOWLEDGEMENTS

This research has been supported by a grant from the Natural Sciences and Engineering Research Council of Canada, and in part by the Ouranos Consortium on Regional Climatology and Adaptation to Climate Change. Thanks to the National Climatic Data Center for providing access to the NARR, and NCEP Global Reanalysis, and to the NOAA Air Resources Laboratory for access to their HYSPLIT trajectory model. Finally, thanks to Environment Canada for access to their online climate information database.

REFERENCES

1. C.S. Cheng *et al., Weather Forecasting*, **19**, 751–768 (2004).
2. F. Mesinger *et al., Bull. Amer. Meteor. Soc.*, **87**, 343–360. (2006)
3. G.I. Huffman, G.A. Norman, *Monthly Weather Review*, **116**, 2172-2182 (1988).
4. G. Ressler, M. Sc. Thesis, McGill University (2010).
5. J.R. Bocchieri, *Monthly Weather Review*, **108**, 596-603 (1980).
6. J.V. Cortinas Jr., Monthly Weather Review, **128**, 3574–3588 (2000).
7. M. Carrera *et al., Journal of Applied Meteorology and Climatology*, **48**, 2341-2361 (2009).
8. P. Bourgouin, *Weather and Forecasting*, **15**, 583-592 (2000).
9. R.M. Rauber *et al., Applied Meteorology*, **40**, 1724–1747 (2001).
10. A. Razy, M. Sc. Thesis, McGill University (2010).
11. S.G. Cober *et al., Journal of Applied Meteorology*, **35**, 2250-2260 (1996).

Assessment of human health risk for Lyme disease in a peri-urban park in southern Québec

Christina Tadiri*[1], Nick Ainsworth[1], Nathaniel de Bono[1], Sonia Gavin[1], Jun Li[1], Katherine Milbers[1], Lien Sardinas[1], Naomi Schwartz[1]

[1]McGill School of Environment, McGill University, 3534 University Street, Montreal, Quebec, Canada H3A 2A7

ABSTRACT

Introduction: Climate change has contributed to the spread of the hard tick *Ixodes scapularis* into increasingly northern latitudes, and subsequently has caused the spread of the Lyme disease causing bacterium, *Borrelia burdorferi*, into these northern areas. The spread of these ticks into the region of southern Québec is highly likely within the near future. As a result, new human populations are being exposed to these ticks and are at risk for contracting Lyme disease. **Intent**: This exploratory study examines the spatial and behavioral factors associated with human activity in Longueuil Regional Park in relation to risk for Lyme disease. **Methods**: We conducted exit surveys of park-goers to determine spatial and behavioral patterns of park use, as well as Lyme disease awareness. **Results and Conclusion**: We found higher awareness of ticks in female park-goers, park-goers over 50, and high-frequency park-goers. Our results, importantly, imply a discrepancy between peoples' awareness of tick bite precautions, and their perception of tick bite risk. We hope that these findings may help future research on the spread of Lyme disease into Canada, as well as in the formulation of public health policy.

KEYWORDS

Lyme disease, human risk assessment, climate change, public health

*Corresponding author:
christina.tadiri@mail.mcgill.ca

Received: 2 January 2011
Revised: 5 March 2011

INTRODUCTION

LYME DISEASE

Lyme disease (LD) is a multi-system pathology caused by the bacterium *Borrelia burgdorferi* in North America *(2)*. The hard tick species *Ixodes scapularis*, commonly known as the deer tick or black-legged tick, carries and transmits the disease. Primary and secondary hosts of the tick are the white-tailed mouse and the white-tailed deer *(3)*, while humans (and other mammals) act as inadvertent hosts. Bacterial transfer (i.e. through a tick bite) between vector and the human host can result in LD.

LD symptoms include fatigue, chills, fever, headache, muscle and joint pain, swollen lymph nodes, and a circular (bulls-eye) rash called *erythema migrans* which appears at the site of the bite *(4)*. If LD is left untreated, central and peripheral nervous system disorders, skin rashes, arthritis and arthritic symptoms, heart

palpitations, and extreme fatigue *(5)* may develop, as well as recurring arthritis and neurological problems *(4)*.

Prevention of LD entails taking simple precautions such as applying insect repellent and minimizing skin exposure while outdoors so as to avoid bites from infected ticks *(6)*. Additionally, experts advise individuals to check their bodies and remove ticks before they attach to the skin, and to consult a physician upon finding any attached ticks *(7–9)*.

CLIMATE CHANGE AND THE SPREAD OF LYME DISEASE

Climate change, paired with anthropogenic land-use change, has led to an increased chance of tick survival and dispersion in southern Québec *(1)*. Until recently, winters in Québec had been harsh enough to combat the spread of ticks *(10)* since the ticks cannot survive winters, where temperatures regularly dip below –7°C*(11)*. However, increasingly warmer winters would lead to a higher survival rate for ticks, and consequently increase the chances of LD transmission. As human populations in North America grow, urban sprawl will likely perpetuate the trends of deforestation and forest fragmentation that will have lasting effects on the dispersion of rodent and deer species *(12)*. The effects of such fragmentation are particularly evident in a peri-urban park setting as Longueuil Regional Park.

Ogden et *al. (13)* created an algorithm based on passive surveillance data that combined vectors, climate change and host species data to determine the chances of the establishment of tick population in certain regions. They concluded that there is a high risk of such establishment in southern Québec and southern Ontario within the next ten years is high. This result implies that LD is a public health concern for Canada, as increased populations of ticks will pose a threat to a population that is perhaps currently unfamiliar with and unprepared for LD.

HUMAN RISK ASSESSMENTS FOR LYME DISEASE

There are currently a wide variety of approaches for conducting human risk assessments for LD. Several have focused solely on quantifying the risk of being bitten by a tick *(14–17)*. Other studies have incorporated a "transmission risk" element into their human risk assessments, where the bacterial seroprevalence in the tick population is also measured, combining the probability of being bitten by a tick with the probability that the tick is a carrier of *B. burgdorferi (18, 19)*. Others have considered risk on a broader scale, identifying environmental characteristics of areas (such as land cover type) that are associated with tick populations in order to create a risk index for an entire region *(20–22)*.

Despite these varied approaches, only a limited number of studies have taken into account both human behaviour and awareness in assessing the risk of LD contraction *(8, 9, 23)*. Recently, a study conducted in the Fôret de Sénart (France) attempted to integrate human and tick spatial distributions as well as human behaviour to develop a more comprehensive assessment of risk *(24)*. Our research has taken a similar approach to assessing risk by additionally evaluating human awareness and activity in a quantitative manner.

LONGUEUIL REGIONAL PARK

The study took place in Longueuil Regional Park (also known as Parc Michel Chartrand) located in Longueuil, Québec. An interview with park staff yielded the following background information: 1) the park encompasses 185 hectares and is bounded by several residential and commercial complexes; 2) due to urban expansion in the area, visitor numbers are increasing, with visitors participating in a wide variety of activities; and 3) within the park, there are several types of vegetation, a wide variety of birds and rodents, and a large population of deer estimated at around 50 individuals. The park's peri-urban setting means that there is an increasing number of park visitors and close interaction with the wildlife; therefore, Longueuil Regional Park is an ideal study site for assessing the risk of contracting LD in a non-endemic area.

RESEARCH QUESTION & HYPOTHESIS

We gathered data with the intent of answering the following question: *What spatial and behavioural factors put the general public at risk for contracting Lyme disease in Longueuil Regional Park?* This project was designed as a descriptive research project. As such, we did not apply a specific hypothesis. The scope of this project was to assemble data in order to frame a picture of the larger relationship between human activity and tick density. This research question carries the implicit assumption that contact with infected ticks is necessary for contracting LD. To answer the above research question, we determined the factors that increase the risk of contracting the disease should the LD pathogen become prevalent in the Longueuil Regional Park tick population.

METHODS

We chose four of the most prominent park exits as points for survey sampling, then determined the number of surveys to administer at each exit based on the proportion of traffic at each exit. Researchers administered surveys verbally in French on one weekday and two weekend afternoons in early November.

The first part of the survey consisted of a user-friendly map of the park on which we asked respondents to trace the route

that they traveled through the park on that specific visit. We then used Geographic Information Systems (GIS, ArcMap version 10) to analyse these data - we examined all traced maps, recorded the number of times each trail segment was used, and then layered this information into a GIS trail map. We also collected spatial data on projected tick distribution (based on land cover type) from a concurrent student-led literature review in the McGill School of Environment (unpublished report), and georeferenced those data into GIS, merging our spatial data with that of the students. Their literature review projected a high correlation between large oak tree areas and high tick densities *(3, 25, 26)*. We defined park areas of high population risk as sites with both frequent human visits and high projected tick densities. Therefore, the intersection of our trail buffer and oak tree areas is where humans were at higher individual risk for contact with ticks. The areas of highest population risk were defined as places where trail segments of high-frequency human visits intersected high tick density areas. To make the trails more visible as well as account for off-trail possibilities, a 10m buffer was applied around the trails.

The second part of the survey was a questionnaire designed to collect the respondent's demographics and behavioural information on that specific park visit. We specifically included questions pertaining to certain behaviours that have been identified in the supporting literature as conducive to tick bites, such as lying in the grass, going off-trail, or coming into contact with wildlife *(7-9)*. Questions regarding knowledge and employment of precautions against tick bites were also included. We organized and analyzed the data collected from the responses using Microsoft Excel 2007 and JMP 8 statistical software. We defined a working null hypothesis (H_0), which is that there was no significant difference in either reported behaviour or reported awareness of tick precautions between complimentary demographic categories (e.g. awareness likelihood of females versus males). We then performed $\chi 2$ analyses with an α-value of 0.05 to test H_1 for all relevant categories.

Finally, we merged data from questionnaires and trail maps using Microsoft Excel 2007, and performed a subgroup analysis of individuals who visited one or more high population risk zones; their behavioural and demographic characteristics were also compared to those of individuals who did not visit a high-risk zone to determine if any significant differences existed.

RESULTS

We identified several trails that represented the highest population risk zones in the park (Fig. 1): trails 3B, 5H, 5F, H5, H6, H7, and H8. We then removed the latter four for two reasons.

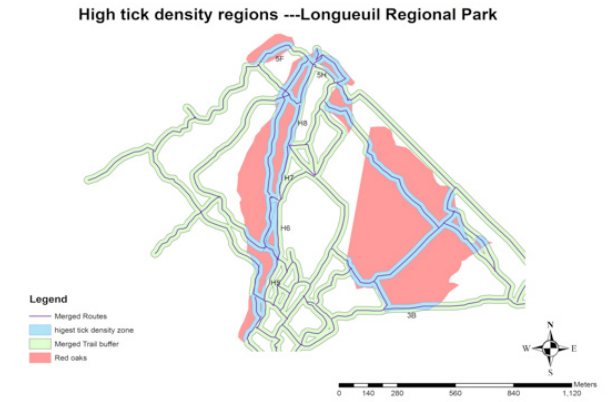

Fig 1. Overlay of high tick density vegetation onto trail map

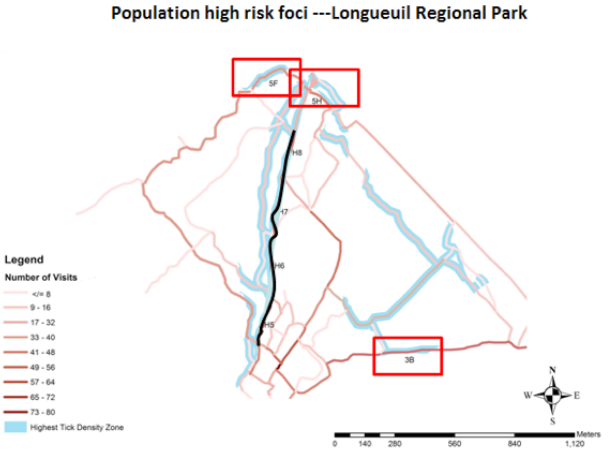

Fig 2. Isolation of high-risk foci. Segments H5, H6, H7 and H8 (black) were excluded from the analysisp

Comparison	Degrees of Freedom	p-value (α = 0.1)2	Direction of awareness
Gender and Tick Awareness (χ^2 contingency test)	1	0.0340	Females > Males
Age (<50 or ≥ 50) and Tick Awareness (χ^2 contingency test)	1	0.0420	50 and over > under 50
Exit Location and Tick Awareness ($\chi 2$ contingency test)	1	0.0660	Adoncour < all others
Frequency of Use and Tick Awareness (χ^2 contingency test)	3	0.0660	More frequent visitor > less frequent
Gender and Mean Age (independent samples T test)	101	0.1471	No relationship

Table 1. Summary of statistically significant results from park survey data

Firstly, these sections fall along the border of two different vegetation types: high tick density coverage (red oak) and low tick density coverage (grass, broad leaf trees, and marshland); this was not a clear indicator of risk. Secondly, these segments of path all belong to the wide *Coeur en mouvement* path, the only path in the park that is paved. Since the risk of contact with ticks on pavement is negligible *(27)*, we determined that this trail did not present significant risk to humans. The final map highlights the three "high-risk foci" that we defined (Fig. 2).

We collected questionnaires from 103 respondents. Within our sample, 45.6% of respondents reported awareness of tick precautions, but only 28.1% reported that they were actively employing any tick precautions on that day. 19.4% of respondents reported going off of the trails and 12.6% reported contact with wildlife. From χ^2 analyses of questionnaire responses, we identified four statistically significant relationships (α=0.1) (Table 1). While we originally set our α-value to 0.05, we have also included results in the $0.05 \leq \alpha \leq 0.1$ range since we feel that these relationships are important in their implications, while we recognize the greater probability of a Type-1 error. We found that females were generally more aware of tick precautions than males (p=0.034, df=1), and that respondents over 50 years of age were also generally more aware than other age groups (p=0.042, df=1). An independent samples t-test confirmed that mean age did not differ significantly between genders (p=0.1471, df=101), implying that these factors independently influence awareness. We also determined that respondents at the largest exit (rue Adoncour) were less likely to be aware of tick precautions (p=0.066, df=1) than those at other exits. Finally, we found a positive correlation between frequency of park use and precaution awareness (p=0.066, df=3).

We isolated three high-risk foci on our map: trail segments that received the highest human use and that were situated in a land-cover type with highest projected tick densities. We identified 57 events where one of these segments was walked on, corresponding to 26 respondents. A comparison of demographical, behavioural, and awareness patterns of the 26 respondents with that of the population frequenting other areas yielded no statistically significant differences.

DISCUSSION

Some of the high-risk activities we identified were not significantly reported within our sample, possibly because of the weather and time of year. For example, only about 8% of respondents reported sitting or lying in grass. We feel that this activity requires further investigation since it is a significant risk factor for contracting LD; however, it may be much more common in the warmer months, also a time when tick populations are more abundant. About 20% of our sample reported going off-trail, indicating that it is fairly common and could be a potential source of population risk. However, we were not able to find a significant relationship between off-trail use and any specific demographic group, nor were we able to determine whether or not our subjects went off-trail in a high-risk area. Thus, based on our data, it is feasible to conclude that all users of the park are at roughly equal potential risk for tick contact and that no particular demographic group or activity is more likely to be associated with any particular area.

Given the relative ease with which LD can be prevented, knowledge of the disease and of precautions against tick bites is crucial in assessing disease risk at both the individual and population level. Since LD has only recently become a reportable disease in Canada (*5*) and the risk is relatively unknown or thought to be negligible, we expected very few of our subjects to be familiar with the disease and/or preventative measures against it. While LD is still fairly rare in southern Québec, our results show that a significant proportion of the population (nearly half) are aware of the disease and of preventative measures. However, we also observed a discrepancy between awareness of precautions and their actual employment of precautions. Less than two-thirds of those who reported being knowledgeable about preventative measures against LD reported taking any precautions; moreover, this value may be inflated due to cold weather encouraging the use of protective clothing. It is also possible that people misunderstood this question and listed the behaviours that they were aware of, even if they were not employing them. For these reasons, the gap between knowledge and behaviour is possibly larger than reported. This discrepancy is consistent with other studies performed in areas where LD is endemic *(23, 28)*. Some of the individual responses we received about employed precautions also indicated misinformation about the disease: this calls into question our reported awareness rate, and raises the possibility that awareness of actual tick precautions may be lower than the survey indicated.

Our results highlighted differences in awareness of tick bite precautions between different demographic groups. First, we found a significantly higher rate of awareness in females than in males, consistent with other reports of LD awareness in the United States *(23)*. Second, we detected an increase in awareness with age. Third, there was a marginally lower rate of awareness at the Adoncour exit (p=0.066, df=1), which is the most-used exit in the park. This difference was not likely a result of variations in frequency of use at the different exits, as frequency of use was not found to vary significantly by exit. This result, along with the demographic representativeness of users of the high-risk areas, reinforces that a general majority of park-goers are likely at risk for tick contact.

Contrary to previous studies in areas in where LD is endemic *(23, 28)*, we established a positive correlation between frequency of park use and awareness of tick precautions. The literature suggests that those knowledgeable about this disease tend to refrain from outdoor activities or avoid parks due to perceived risk of contraction *(23)*, which would negatively bias our awareness results. The positive correlation we identified could be explained by a low perception of risk for LD. It may be that subjects are (correctly) aware that the risk is currently negligible, and therefore use the park. Nonetheless, the low perception of LD risk coupled with the fact that ticks (albeit few) have been found in the park and that their numbers have been increasing in the area *(1)*, could constitute a key area for future public health interventions. If LD prevalence increases, public health measures will need to make the public aware of the actual risk--not simply precautions--in order to increase the employment of precautions.

CONCLUSION

With one exception, *(24)*, there are very few comprehensive assessments of LD risk based on human and tick distribution, as well as human behaviour and awareness. Our study is a preliminary attempt at addressing this deficiency in the literature. Since LD is relatively new to the area, now is the opportune time to be performing such risk assessments.

This project aimed to characterize the spatial patterns of future LD population risk and to elucidate some of the most pertinent factors that determine individual risk. We have also considered how these data might guide both policy planning and future research in a similar vein.

To better understand the human risk for LD in the future, it is important that future studies gather highly representative samples. The principal operational challenge for our research was the time of year at which it was conducted: we would strongly recommend that future work in this region be conducted during the summer months when response rates, activity breadth, and the feasibility of a larger sample size will all benefit from warmer temperatures.

Our results, while potentially significant, are preliminary. Thus, southern Québec in particular needs to be further studied before regional trends can begin to be extrapolated, and certainly before region- or province-wide public health action can be undertaken. We hope that future studies in this area can build upon these data, and also refine the methodology.

ACKNOWLEDGEMENTS

We would like to thank Dr. Nick Ogden from the Zoonoses division of the Public Health Agency of Canada and his post-doctoral student Dr. Patrick Leighton for giving us this project, the McGill School of Environment (MSE) for funding and the six students from the MSE for sharing their literature review and data. We would also like to thank Dr. Bruce Case (Pathology, McGill University) for his guidance, Dr. Elena Bennet (Geography, McGill University) for her help and Ms. Christine Provost (Municipality of Longeueil) for sharing information and geospatial maps pertaining to Longueuil Regional Park.

REFERENCES

1. N. H. Ogden *et al.*, Environmental Health Perspectives **118**, 909 (Jul, 2010).
2. A. Barbour, D. Fish, *Science* **260**, 1610 (June 11, 1993, 1993).
3. D. H. Walker *et al., JAMA* **275**, 463 (February 14, 1996, 1996).
4. CDC, in *Division of Vector-Borne Infectious Diseases*. (2007), vol. 2010.
5. PHAC. (2010), vol. 2010.
6. CDC, in *Division of Vector-Borne Infectious Diseases.* (CDC, 2010), vol. 2010.
7. L. H. Gould, R. S. Nelson, *Vector-Borne and Zoonotic Diseases* **8**, 769 (2008).
8. R. S. Lane *et al., American Journal of Epidemiology* **136**, 1358 (December 1, 1992).
9. G. Smith, E. P. Wileyto, R. B. Hopkins, B. R. Cherry, J. P. Maher, *Public Health Reports* **116**, 146 (2001).
10. N. H. Ogden *et al., Applied and Environmental Microbiology* **74**, 1780 (2008).
11. J. A. Patz, S. H. Olson, C. K. Uejio, H. K. Gibbs, *Medical Clinics of North America* **92**, 1473 (2008).
12. K. LoGiudice, R. S. Ostfeld, K. A. Schmidt, F. Keesing, *Proceedings of the National Academy of Sciences of the United States of America* **100**, 567 (2003).
13. N. H. Ogden *et al., International Journal of Health Geographics* **7**, 15 (2008).
14. R. S. Lane, A*m J Trop Med Hyg* **55**, 165 (August 1, 1996, 1996).
15. R. C. Falco, D. Fish, *American Journal of Public Health* **79**, 12 (Jan, 1989).
16. A. Altobelli *et al., International Journal of Medical Microbiology* **298**, 125 (Sep, 2008).
17. J. Piesman, L. Eisen, *Annual Review of Entomology* **53**, 323 (2008).
18. H. S. Ginsberg, *American Journal of Epidemiology* **138**, 65 (Jul 1, 1993).
19. P. W. Rand, E. H. Lacombe, R. P. Smith, K. Gensheimer, D. T. Dennis, *American Journal of Tropical Medicine and Hygiene* **55**, 160 (Aug, 1996).
20. T. L. Schulze, R. C. Taylor, G. C. Taylor, E. M. Bosler, *American Journal of Public Health* **81**, 714 (Jun, 1991).

21. M. E. Killilea, A. Swei, R. S. Lane, C. J. Briggs, R. S. Ostfeld, *Ecohealth* **5**, 167 (Jun, 2008).
22. G. E. Glass *et al.*, *American Journal of Public Health* **85**, 944 (Jul, 1995).
23. W. Hallman, N. Weinstein, S. Kadakia, C. Chess, *Environment and Behavior* **27**, 437 (Jul, 1995).
24. O. Thomas, Masters, Université de Paris (2010).
25. A. Lindström, T. G. T. Jaenson, *Journal of Medical Entomology* **40**, 375 (2003).
26. A. R. Walker, M. P. Alberdi, *Medical and Veterinary Entomology* **15**, 40 (2001).
27. T. J. Daniels, R. C. Falco, I. Schwartz, S. Varde, R. G. Robbins, *Emerging Infectious Diseases* **3**, 353 (Jul-Sep, 1997).
28. S. W. Brown, M. L. Cartter, J. L. Hadler, *American Medical Association Archives of Dermatology* **128**, (1992).

A call for submissions

McGill Science Undergraduate Research Journal

We publish research articles and review papers by students at the undergraduate level. Articles are selected on a competitive peer-review basis. We also seek authors for science interest pieces and feature articles.

Submit your article by **January 1st, 2012.**

To find our guidelines and past volumes
To apply to be on the MSURJ editorial board
Visit **http://msurj.mcgill.ca**
Contact **mcgillsurj@gmail.com**